https://doi.org/10.5194/egusphere-2025-1752
Preprint. Discussion started: 25 April 2025

Precipitation, Moisture Sources and Transport Pathways associated with Summertime North Atlantic Deep Cyclones

Rikke Stoffels[1,2,3], Imme Benedict[3], Lukas Papritz[4], Frank Selten[2], Chris Weijenborg[3]

[1]Institute for Environmental Studies, Vrije Universiteit Amsterdam, Amsterdam, the Netherlands
[2]Royal Netherlands Meteorological Institute (KNMI), de Bilt, the Netherlands
[3]Meteorology and Air Quality Group, Wageningen University and Research, Wageningen, the Netherlands
[4]Institute for Atmospheric and Climate Science, ETH Zurich, Zurich, Switzerland

Correspondence to: Rikke Stoffels (r.stoffels@vu.nl)

Abstract. Extratropical cyclones are essential for redistributing moisture from lower latitudes to the poles, and are known for their ability to produce (extreme) precipitation. While wintertime extratropical cyclones have been studied in great detail, little is known about these systems in summer. Therefore, the objective of this study is to improve our understanding of how summertime extratropical cyclones shape the characteristics of the water cycle, focusing on their moisture sources and the transport of moisture to cyclone centers. For this purpose, 8-day backward trajectories are calculated for all air parcels in the vicinity of cyclone centers, for a subset of the most intense summertime cyclones over the North Atlantic. Subsequently, moisture uptakes along the trajectories of precipitating air parcels are identified using the moisture source diagnostic WaterSip. Using this approach, it is found that the bulk of the precipitation associated with summertime cyclones falls close to the cyclone center in the warm conveyor belt (WCB) and along the fronts, mainly during the cyclone's intensification phase. The origin of this moisture correspond to areas of high ocean evaporation, with significant hotspots on the warm side of the Gulf Stream Front. In addition, some continental sources are found, especially for cyclones in the Labrador Sea. Moisture uptake occurs primarily in regions where the strong SST gradient induces intense ocean evaporation and during cold-air advection within the cyclone's cold sector, where oceanic evaporation is enhanced due to the strong air-sea temperature contrast. The moisture accumulated in the cold sector of the cyclone does not necessarily contribute to precipitation in its own center, but it can act as a source of moisture for a subsequent cyclone. As cyclones mature, the dominant moisture sources shift from remote regions to more localized sources, but the atmospheric residence time of moisture of about four days remains approximately the same throughout the cyclone life cycle. This is because the decrease in source distance is compensated by weaker winds and less strong convergence. Overall, these results are fairly similar to those found in a previous study for winter cyclones, although in winter there is more moisture exchange between primary and secondary cyclones, and stronger vertical ascent in the WCB. Summer cyclones, on the other hand, are distinguished by their greater moisture supply from continental sources, and the significant influence from cyclones of tropical origin undergoing extratropical transition.

Short summary. Summertime North Atlantic storms bring heavy rainfall, especially near their centers and along their fronts. By tracking precipitating air parcels back in time we find that the moisture comes from areas of strong ocean evaporation, with

https://doi.org/10.5194/egusphere-2025-1752
Preprint. Discussion started: 25 April 2025

hotspots in the Gulf Stream region. We also find that sometimes evaporation in a previous storm can contribute to rainfall in the next. Unlike in winter, summer storms also draw moisture from land, and their properties are partly shaped by former tropical storms.

1 Introduction

Extratropical cyclones make up an important component of the global atmospheric circulation by redistributing energy, moisture and momentum from lower latitudes to the polar regions (Field and Wood, 2007; Neu et al., 2013; Papritz et al., 2021). Cyclones enhance atmospheric moisture by promoting evaporation from various surfaces such as the land, oceans, lakes and rivers. Once the moisture enters the boundary layer, the cyclones facilitate transport over long distances during which the moisture is subject to mixing and convection, as well as synoptic and global-scale motions (Boutle et al., 2011). At the same time, they also act as an important sink for atmospheric moisture by returning it to the surface through associated (heavy) precipitation, which can have severe impacts on society. For instance, the extreme rainfall associated with cyclones can result in flood events, and occasionally they have been associated with other natural disasters such as storm surges or wind gust-related damage (Dacre et al., 2019; Laurila et al., 2021; Messmer and Simmonds, 2021).

Understanding the processes that govern precipitation in extratropical cyclones is essential, as several studies (e.g. Konstali et al., 2024; Pfahl and Wernli, 2012) have found that cyclones within the midlatitude storm track region account for more than 80% of the precipitation extremes in the Northern Hemisphere, if precipitation in the accompanying fronts is included. Given their significant role, accurately forecasting these precipitation extremes and the representation of extratropical cyclones in climate models has received increasing scientific attention and remains a key component of the work of the Intergovernmental Panel on Climate Change (IPCC) (Catto, 2016). However, to improve our understanding of these processes, a comprehensive understanding of the role of extratropical cyclones in the atmospheric water cycle — throughout their life cycle — is first required. Despite their influence on midlatitude weather and climate, there is still much to learn about the role of extratropical cyclones in the atmospheric water cycle. This is especially true for summertime cyclones, which have received less scientific attention than their winter equivalents (Mesquita et al., 2008).

Previous research on extratropical cyclones highlights the fundamental differences between these systems and their tropical counterparts. Precipitation in tropical cyclones is concentrated near the storm's core and is generally more intense, due to a combination of high sea surface temperatures (SSTs) and deep convection. Conversely, extratropical cyclones are driven by baroclinicity and have characteristic frontal structures (Ahrens, 2009; Chang and Song, 2006; Eckhardt et al., 2004). Within these systems most of the precipitation falls in the region of warm air between the cold and warm front that extends from the cyclone center in a northeasterly direction, also called the warm sector (Ahrens, 2009; Chang and Song, 2006; Papritz et al., 2021). Here, air masses converge and ascend, causing moisture to condense and rain out. This location coincides with the location of the warm conveyor belt (WCB), a rising airflow characterized by intense latent heat release and large amounts of precipitation. The WCB is oriented parallel to the cold front and typically propagates poleward (Boutle et al., 2011; Catto,

https://doi.org/10.5194/egusphere-2025-1752
Preprint. Discussion started: 25 April 2025

2016). Over time, large-scale vertical motions lift the WCB above the warm front, after which it splits into two branches: one wrapping cyclonically northward around the low-pressure center and the other wrapping anticyclonically in an easterly direction (Boutle et al., 2010). As a result, the spatial extent of the WCB not only consists of a diagonal air flow, but also stretches horizontally in the northern outflow region, creating the characteristic comma-shaped structure described in the Norwegian model (Bjerknes and Solberg, 1922) and the T-bone structure of the Shapiro-Keyser model (Shapiro and Keyser, 1990). In the WCB, it is possible for moisture to be advected from the boundary layer to the upper troposphere by a large-scale ascent in roughly two days (Eckhardt et al., 2004). Hence, WCBs contribute significantly more to the moisture content in the upper troposphere than shallow convective processes and are therefore considered the main sink of precipitable water in the atmosphere (Boutle et al., 2011; Sodemann and Stohl, 2013). According to Eckhardt et al. (2004) and Pfahl et al. (2014), the WCB and extratropical cyclones are often linked, and, in addition, the WCB is actually able to influence the dynamics of the cyclones.

The amount of precipitation that is generated within a cyclone depends on the strength of the vertical motions in the WCB, as well as the amount of moisture transported to the cyclone center. Sodemann and Stohl (2013) found that water vapour by means of atmospheric rivers (ARs) had been transported from remote southerly source regions to the center of the cyclones at the end of the North Atlantic storm track, and then induced intense precipitation over western Scandinavia due to steep orographic rise. ARs are narrow filaments of high vertically integrated moisture that can act as a moisture supply for extratropical cyclones. Since ARs are not tied to one specific cyclone and can exist even without cyclone airflows, a clear distinction must be made between WCBs and ARs (Dacre et al., 2019; Eckhardt et al., 2004; Knippertz et al., 2018). However, this does not mean that ARs cannot be associated with precipitation falling at the cyclone center. For example, ARs are capable of feeding multiple WCBs from individual cyclones, and appear to be the source of moisture in several cases (both in the North Atlantic and the Pacific ocean) where cyclones encounter steep orographic rises. In the study by Papritz et al. (2021) on the moisture sources and transport pathways of precipitating waters of wintertime North Atlantic deep cyclones, subtropical moisture plumes in the form of ARs are also recognized as potential source areas, especially in the early phase of cyclone development. Additionally, Papritz et al. (2021) suggest that evaporation from the ocean surface, triggered when cold polar air passes over relatively warmer ocean currents, supplies the cyclone with moisture. Ultimately, they identify the cold sector of a preceding low-pressure system as the predominant moisture source for wintertime North Atlantic deep cyclones. From there, moisture is transported over a relatively short distance to the center of another developing cyclone following the same track, resulting in a short moisture residence time. This phenomenon, in which a primary cyclone is succeeded by several secondary cyclones forming in succession, is known as a cyclone family or cluster (Bjerknes and Solberg, 1922; Priestley et al., 2020) and is particularly common in winter (Weijenborg and Spengler, 2024). Geographically, Papritz et al. (2021) found that moisture uptakes are mainly restricted to the western North Atlantic and are concentrated on the warm side of the Gulf Stream Front and its extension.

The pathways and sources of the precipitating waters in extratropical cyclones during the summer months remain largely unexplored. In winter, a stronger equator-to-pole temperature gradient enhances the jet stream, resulting in higher wind speeds

https://doi.org/10.5194/egusphere-2025-1752
Preprint. Discussion started: 25 April 2025

and enhanced vertical motions within the WCB. In summer, weaker temperature gradients may reduce WCB strength, but stronger latent heat fluxes from the warmer ocean surface could provide additional moisture. This raises critical questions about how moisture pathways, such as those from the warm side of the Gulf Stream Front or even from the subtropics, play a greater role in generating precipitation within summertime extratropical cyclones.

Understanding the behavior of summertime cyclones is essential, as it will allow us to discern what makes these systems unique compared to their winter counterparts. However, before we can explore the differences, we must first establish a solid understanding of what drives precipitation and moisture uptake in the summer months. This study, therefore, aims to address this knowledge gap by studying the precipitation characteristics, moisture sources, and transport pathways of summertime North Atlantic deep cyclones. We specifically focus on how these components of the cyclone-related water cycle change throughout the cyclone life cycle, and across different subregions within the North Atlantic. The following research questions will be addressed.

Q1: What is the spatial distribution of precipitation within and around the cyclone center?

Q2: What are the geographical and cyclone-relative moisture sources of the precipitating waters?

Q3: In which dynamical environment do moisture uptakes take place?

Q4: How do the uptake and moisture transport characteristics change throughout the life cycle of a cyclone?

Answers to these questions will be sought by identifying the precipitating waters for a set of 688 cyclones and tracing their origins backwards using a Lagrangian approach. Compared to an Eulerian approach, which is also suitable for constructing a moisture budget (e.g. van der Ent and Tuinenburg, 2017), the advantage of the Lagrangian approach is that it allows for the quantification of moisture uptakes along air parcel trajectories and enables the distinction between different air streams (Gimeno et al., 2012; Pérez-Alarcón et al., 2022). The North Atlantic has been chosen as a study region for the following reasons: (1) Moisture uptakes from the ocean surface appear to have a significant contribution to the precipitation that is generated, (2) the results can be compared with results from previous research, as the North Atlantic has been studied several times before (e.g. Chang and Song, 2006), and (3) difficult features such as orography and roughness, both of which are induced by the transition from land to sea (Field and Wood, 2007), can be disregarded. In addition, we focus on deep cyclones, since they generate the most heavy precipitation.

The study is structured as follows. In section 2, the dataset is introduced, the methodology for selecting a subset of the most intense North Atlantic cyclones is explained, and the trajectory calculation tool and the moisture source identification process are described. Section 3 presents a detailed case study of a selected cyclone over the East Atlantic, providing insight into the underlying processes. Next, a climatological analysis of the cyclone-related water cycle associated with all 688 cyclones is presented. To that end, the cyclone precipitation is first discussed, followed by an overview of the moisture sources and transport pathways of these precipitating waters. The paper is concluded by a discussion and final remarks in section 5, focusing on what distinguishes extratropical cyclones that occur during summer from their winter counterparts.

https://doi.org/10.5194/egusphere-2025-1752
Preprint. Discussion started: 25 April 2025

2 Methodology

2.1 ERA5 reanalysis dataset

The analyses presented in this study are based on the ERA5 reanalysis dataset, which is the most recent reanalysis released by the European Centre for Medium-Range Weather Forecasts (ECMWF; Hersbach et al., 2020). For this study, we obtain data at a horizontal resolution of 0.5° x 0.5° for all extended summers (May-September; MJJAS) between 1980 and 2021, on both single levels and model levels. The variables we obtain on single levels are sea surface temperature (SST), surface evaporation, convective and large-scale precipitation, surface pressure, mean sea level pressure (MSLP) and boundary layer height. Additionally, we retrieve the variables (potential) temperature, specific humidity, and three-dimensional wind fields on a selection of model levels extending from the surface (level 137, lower boundary) to 29 hPa (level 40, upper boundary). By using precipitation data from ERA5 reanalysis, it is possible to study precipitation during different phases of the cyclone life cycle, as reanalysis provides measurements of global coverage with high temporal resolution, whereas most satellite products do not (Pfahl and Sprenger, 2016). Moreover, ERA5 is good at resolving the large-scale atmospheric processes, while convective precipitation relies on parameterizations (Lavers et al., 2022). Therefore, given that precipitation in the extratropical region is predominantly driven by large-scale dynamics, the ERA5 dataset is well-suited for this study.

2.2 Identification and selection of North Atlantic deep cyclones

We identify individual cyclone tracks that developed during MJJAS using the cyclone identification and tracking scheme by Sprenger et al. (2017), which is an improved version of the one initially developed by Wernli and Schwierz (2006). It is one of many methods used to detect and track flow features such as extratropical cyclones, which typically use MSLP or lower-tropospheric vorticity as their base metric but vary in their specific methodology. A method comparison study by Neu et al. (2013) revealed that the scheme used in this study detects a number of cyclones that is similar to the average of all methods and is not an outlier.

The tracking scheme automatically identifies cyclone centers by finding local minima in the gridded hourly MSLP fields, while the cyclone edges are determined as the outermost closed MSLP contour that encloses only the minimum under consideration using a contour search algorithm with a sampling interval of 0.5 hPa (for more details, see Wernli and Schwierz (2006)). Once identified, the cyclones are tracked over time and their coordinates and pressure are recorded.

Subsequently, a subset of the global cyclone tracks is created, comprising exclusively North Atlantic deep cyclones. To this end, the cyclone depth is calculated at hourly intervals along each cyclone track, which is defined as the pressure difference between the cyclone center and the cyclone edge and is a measure of the cyclone's intensity. Thereafter, a new time axis relative to the cyclone life cycle is defined. The time axis is centered around the time of the cyclone's maximum depth, denoted by $t = 0$ h. The time period where $t < 0$ h then represents the intensification phase, while $t > 0$ h, represents the decay phase. Using the cyclone depth as a measure of intensity and the relative time, two selection criteria are imposed: (1) a cyclone must reach its maximum intensity within the North Atlantic region (cf. Fig. 1), and (2) its track length must extend from at least $t =$

https://doi.org/10.5194/egusphere-2025-1752
Preprint. Discussion started: 25 April 2025

-24 h to t = 24 h. In this way, we select a subset of the cyclones located in the geographical region of interest, characterized by a well-defined intensification and decay phase, thereby delineating a distinct life cycle. Single cyclones that split into separate features, or systems that merge with another cyclone are excluded by the second criterion, as such features have an intensification or decay phase that is less than 24 hours (Neu et al., 2013; Papritz et al., 2021). In addition, we exclude cases where the track length in October exceeds that in September or where the cyclone reaches its maximum intensity in October, as these cyclones already begin to exhibit wintertime characteristics due to increased baroclinicity.

For all North Atlantic cyclones with a sufficient track length (3810 tracks), the maximum depth ranges from 2 to nearly 70 hPa, with a mean of 16.8 hPa. The distribution is strongly skewed, with a tail towards higher maximum intensities (Fig. 1e). Since this study focuses on the cyclone-related water cycle, the analysis is further limited to the most intense cyclones that produce the largest precipitation (Pfahl and Sprenger, 2016). To this end, a third and final criterion is used. Only those tracks with a maximum cyclone depth exceeding the 80th percentile threshold value are selected. As a result, 688 cyclone tracks are obtained and are divided into four groups based on the location where they reach their maximum depth: the Gulf Stream region (86 tracks), the Labrador Sea (105 tracks), the East Atlantic (231 tracks), and the Nordic Seas (266 tracks) (Fig. 1a-d). It should be noted that cyclone tracks may extend beyond the respective region where they reach their maximum depth, at any point in their lifetime. For instance, many cyclones originate over the North American continent or originate in the tropics before extending eastward along the North Atlantic storm track, with some eventually making landfall in Europe. Consequently, the selection of summer extratropical cyclones exhibit strong movement. Using the definition of a moving cyclone proposed by Eckhardt et al. (2004), the selection is limited to three stationary cyclones, while the remaining 685 cyclones all travel more than 1000 km during their lifetime and intensify by more than 10 hPa.

In our subset of cyclones, 46 have tropical origins, which we define as originating at or below 23° N, and then undergo extratropical transition (28 in the Gulf Stream region, 3 in the Labrador Sea, 15 in the East Atlantic). Given the tendency of tropical cyclones to exhibit greater intensity compared to extratropical cyclones, they shift the overall distribution of maximum cyclone depth towards higher intensity values (Fig. A1). This is particularly true in the Gulf Stream region, which also has the highest percentage of cyclones of tropical origin (~33%). Cyclones that originate in the tropics and are among the 20% strongest cyclones in the extratropics are not observed in winter, making them unique. Therefore, including these cyclones in our study is both necessary and particularly interesting.

https://doi.org/10.5194/egusphere-2025-1752
Preprint. Discussion started: 25 April 2025

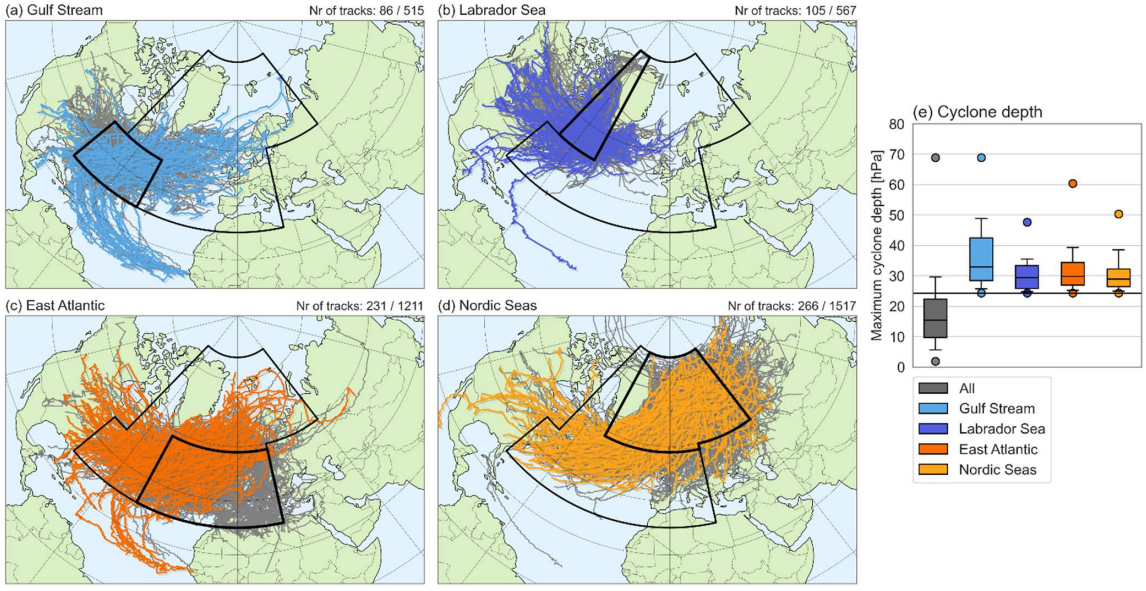

Figure 1: Selected tracks in (a) the Gulf Stream region, (b) the Labrador Sea, (c) the East Atlantic Ocean, and (d) the Nordic Seas. The selected tracks are highlighted in colour and meet the three selection criteria for duration, intensity and location. At the top right of each panel, the number of cyclone tracks that have been selected are given as the proportion relative to the total of tracks within each of the four subregions. (e) The distribution of the maximum depth of all North Atlantic cyclones with a distinct life cycle (grey) and of the selected cyclones in the four subregions (other colours). The black horizontal line represents the threshold of the 80th percentile of all tracks. In addition, the whiskers indicate the 10th-90th percentile range, and the dots show maxima and minima.

2.3 Calculation of the backward trajectories

The precipitating waters of each summertime cyclone are traced back in time to identify the moisture sources. This is achieved by calculating kinematic backward trajectories of air parcels surrounding the cyclone center every three hours within the time interval of t = -24 h to t = 24 h. The trajectories are computed using the Lagrangian Analysis Tool (LAGRANTO; Sprenger and Wernli, 2015), which employs three-dimensional gridded wind fields on model levels and surface pressure data. A detailed description of the data structure expected by LAGRANTO is given in Sprenger and Wernli (2015).

The LAGRANTO methodology involves a three-step procedure. In the first step, initial grid points are defined from where the air parcels are released. The number of possible grid points is constrained by the requirement that they be initialized on an equidistant grid having a mesh size of 50 km in the horizontal direction and 25 hPa in the vertical direction, extending from the surface up to 400 hPa. Furthermore, the starting positions have to be located within a circle with a radius of 500 km around the center of the cyclone (Papritz et al., 2021). The size of the radius around the cyclone center was chosen and justified by Papritz et al. (2021), and is based on the attempt to include most of the precipitation in the cyclone core that is driven by dynamical ascent, and to exclude precipitation located further away from the cyclone center that might be triggered by orography and frontal circulation. In the second step, eight-day backward trajectories are calculated from these positions

https://doi.org/10.5194/egusphere-2025-1752
Preprint. Discussion started: 25 April 2025

(illustrated by grey dots in Fig. 2). The number of days is chosen based on three factors: (1) computational cost and computer power, (2) numerical accuracy, and (3) LAGRANTO's ability to allocate a significant proportion of precipitation to the right moisture sources. Finally, various atmospheric variables, including (potential) temperature, specific humidity, relative humidity, the boundary layer height and the latent heating rate are traced along these trajectories. The latent heating rate is estimated by LAGRANTO from changes in specific humidity, while the other variables are obtained from the ERA5 data set. Using these variables, the moisture budget of the air parcel can be constructed by applying the moisture source diagnostic WaterSip (Sodemann et al.; 2008).

2.4 Diagnosis of the moisture uptakes

In this study, we employ the Lagrangian moisture source diagnostic WaterSip to identify the moisture sources (Sodemann, 2025). The tool needs backward trajectories calculated by a trajectory calculation tool such as LAGRANTO as input, and provides source, transport and arrival properties of the moisture. We initiate simulations for each cyclone following the methodology described by Sodemann et al. (2008), as outlined below.

Since we are interested in the moisture sources of precipitation, we first select precipitating trajectories, defined as trajectories where the relative humidity (RH) exceeds 80% at the trajectory start (t = 0 h), and where a significant amount of moisture is lost during the first timestep ($\Delta q < -0.1$ g kg^{-1} 3h^{-1}). The RH threshold aligns with the parameterisation of the ECMWF model, which assumes the presence of clouds from which precipitation falls at a RH above 80% (Sodemann et al., 2008). The two criteria have also been employed by Papritz et al. (2021), thereby facilitating a comparison of our results for the summer and theirs for winter.

In order to analyse the evaporation and precipitation events experienced by an air parcel, the changes in specific humidity are evaluated along each of the remaining trajectories. Increases in specific humidity indicate moisture uptakes, while decreases (before reaching the start point of the trajectory) suggest intermediate precipitation. Assuming that (1) the integrity of these air parcels is maintained over a period of several days, (2) interactions with neighbouring parcels can be neglected, and (3) either evaporation or precipitation dominates during the 3-hour interval, the sign of Δq indicates which process occurs during a given part of the trajectory (Sodemann et al., 2008). To avoid including small fluctuations in the specific humidity that do not correspond to actual evaporation or precipitation events, a threshold value of 0.075 g kg^{-1} 3h^{-1} is applied. Once all the moisture uptake locations are identified, the absolute uptake amount is translated into a moisture source footprint for each time step between -24 h and 24 h. Additionally, the fractional contribution of each uptake event along the trajectory to the precipitation at the arrival location is determined. The sum of these fractional contributions then yields the fraction of the estimated precipitation at the arrival location that can be attributed to the identified origins (Sodemann et al., 2008). Besides this accounted fraction, WaterSip also provides source, transport, and arrival properties for each trajectory. Source properties are determined as the precipitation-weighted mean of all moisture uptake locations. A similar weighting approach is applied to obtain the mean source distance and the mean accounted fraction over all trajectories of a given cyclone at a given time step, ensuring that trajectories with higher precipitation rates have a greater influence on the mean values.

https://doi.org/10.5194/egusphere-2025-1752
Preprint. Discussion started: 25 April 2025

WaterSip makes a distinction between moisture uptakes within the near-surface boundary layer and higher up in the free troposphere. Uptakes in the boundary layer are attributed to surface evaporation, whereas uptakes in the free troposphere may result from subgrid-scale convective ventilation or the evaporation of precipitation (Papritz et al., 2021). By summing these fractions, we obtain a more complete picture of the total moisture uptake during transport.

Figure 2 shows an example of a LAGRANTO trajectory for a particular cyclone and illustrates the WaterSip methodology. Along the trajectory there are two moisture uptakes of almost similar amounts at t = -168 h and t = -48 h, as well as an intermittent precipitation event at t = -96 h. The uptake event at t = -48 h fully contributes to the precipitation in the cyclone center since there is no precipitation event between t = -48 h and t = 0 h. In contrast, the moisture that the air parcel has gained at t = -168 h partly precipitates during the intermittent precipitation event, and will have a smaller contribution to the precipitation at the trajectory start.

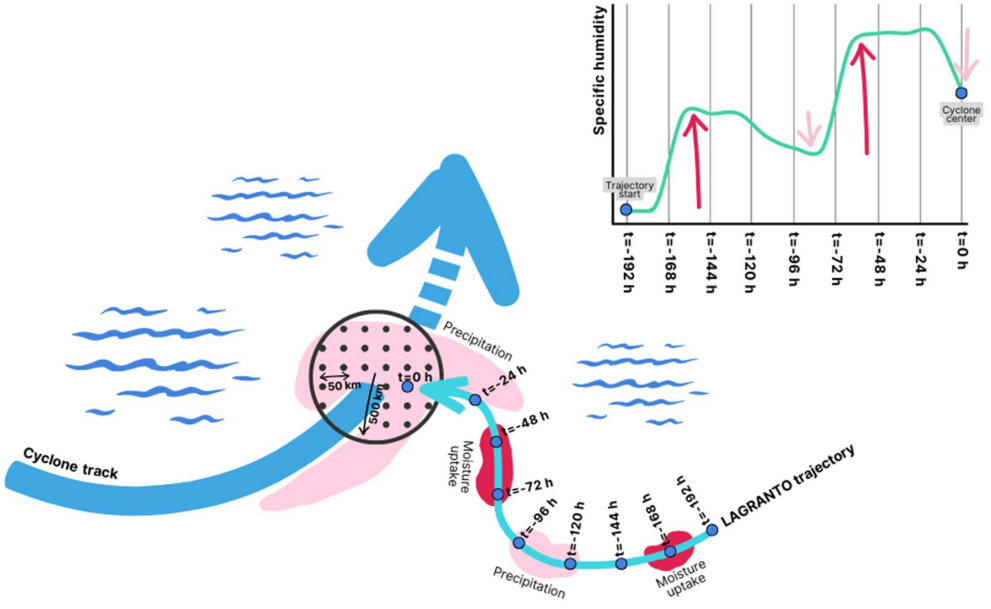

Figure 2: Illustration clarifying the principle of the moisture source diagnostics applied to the LAGRANTO backward trajectories. The blue arrow shows the cyclone track, from which, at a given time, precipitating air parcels that are within a 500 km radius of the cyclone center (grey circle) are tracked backward in time. The light blue arrow shows a possible trajectory that has been calculated by LAGRANTO and will be evaluated by WaterSip. The light pink patches indicate (intermittent) precipitation and the dark pink patches indicate evaporation along the trajectory. The top diagram shows the change in specific humidity over time along the trajectory shown by the light blue arrow, due to the precipitation events (light pink arrows) and evaporation events (dark pink arrows). Figure is adapted from Papritz et al. (2021).

https://doi.org/10.5194/egusphere-2025-1752
Preprint. Discussion started: 25 April 2025

3. Case study of an East Atlantic cyclone

We begin this study with a detailed analysis of a randomly selected case study over the East Atlantic. Studying this case helps clarifying the underlying processes that shape the cyclone-related water cycle and the mechanisms by which moisture is transported into the center of the cyclone, which will ultimately help in the interpretation of the climatological analyses. Although this cyclone was chosen arbitrarily, its landfall in Europe makes it particularly relevant, as such cyclones can have significant regional impacts.

3.1 Synoptic flow evolution

On 4 May 2019, at 23:00 UTC, a cyclone developed in the Gulf Stream region as a secondary cyclone that is part of a cyclone cluster. Over the next two and a half days, the cyclone intensified and travelled to the East Atlantic, where it attained a maximum depth of 35.2 hPa. The decay phase lasted just over two days, during which the cyclone made landfall in Europe. The maximum depth of this cyclone falls within the interquartile range of the selected intense East Atlantic cyclones (cf. Fig. 1e), and it has a representative amount and timing of precipitation, with most precipitation falling during the intensification phase (not shown). Therefore, this cyclone can be considered a typical deep East Atlantic cyclone.

Figures 3 and 4 show the synoptic flow evolution prior to and during the development of the East Atlantic cyclone. In the three days prior to the cyclone attaining its maximum depth, the presence of another preceding cyclone was observed (C1 in Fig. 3 and 4). The rapid formation of multiple cyclones in succession, so-called cyclone clustering, is a common feature observed over the North Atlantic. According to Priestley et al. (2020) and Weijenborg and Spengler (2024), more than 50% of cyclones along the main North Atlantic storm track are part of a cyclone cluster. While this behaviour has primarily been studied in the context of winter cyclones, the present case illustrates that such cyclone clusters also occur in summer.

The dynamical flow pattern in the days before the secondary cyclone developed was predominantly influenced by the primary cyclone, as shown in Fig. 3. This figure shows 12-hourly maps of 900 hPa sea–air potential temperature difference for t = -72 h to t = 24 h. The passage of the primary cyclone is followed by the presence of a region of strongly positive sea–air potential temperature difference, i.e., cold-air advection over a warm ocean surface, particularly in the hours leading up to the development of the secondary cyclone (Fig. 3a-c). This region is surrounded by strongly negative sea–air potential temperature difference, i.e., warm-air advection. The region of cold-air advection represents the cyclone's cold sector, characterized by strong upward fluxes of sensible and latent heat (e.g., Papritz et al. 2015), as also confirmed by Fig. 4a-c. To the west of this region of intense surface evaporation, we observe the genesis of the secondary cyclone (Fig. 3c).

A priori it remains unclear whether the moisture injected into the atmosphere in the primary cyclone's cold sector directly contributes to precipitation in the secondary cyclone. However, assuming that relatively weak winds can keep the moisture in place, and the fact that the secondary cyclone propagates into and across the region of high surface evaporation associated with the primary cyclone, it is plausible that evaporation in the cold sector of a preceding cyclone can eventually feed a subsequent cyclone with moisture.

https://doi.org/10.5194/egusphere-2025-1752
Preprint. Discussion started: 25 April 2025

Another region of high evaporation is located to the south the secondary cyclone, where a positive sea–air potential temperature difference coincides with the subtropical high. Here, relatively cold, dry air descends over a warmer ocean surface, enhancing evaporation. The positioning of the cyclone and anticyclone induces easterly winds along the Gulf Stream Front, a region characterized by a sharp transition from negative to positive sea-air temperature differences due to the strong SST gradient. As a result, intense evaporation occurs on the warm side of the Gulf Stream Front, particularly between t = −12 h and t = 12 h (Fig. 4f-h). Given the prevailing wind direction, this region contributes to the secondary cyclone's precipitation as well.

Additional regions of elevated surface evaporation seen in Fig. 4 include the land surface and cold-air advection within the cyclone's own cold sector. However, the latter becomes prominent only later in the cyclone's life cycle, from t = 0 h onward. To determine whether these evaporation hotspots indeed contribute to precipitation within the cyclone center, we will in the following section consider the moisture sources for this case.

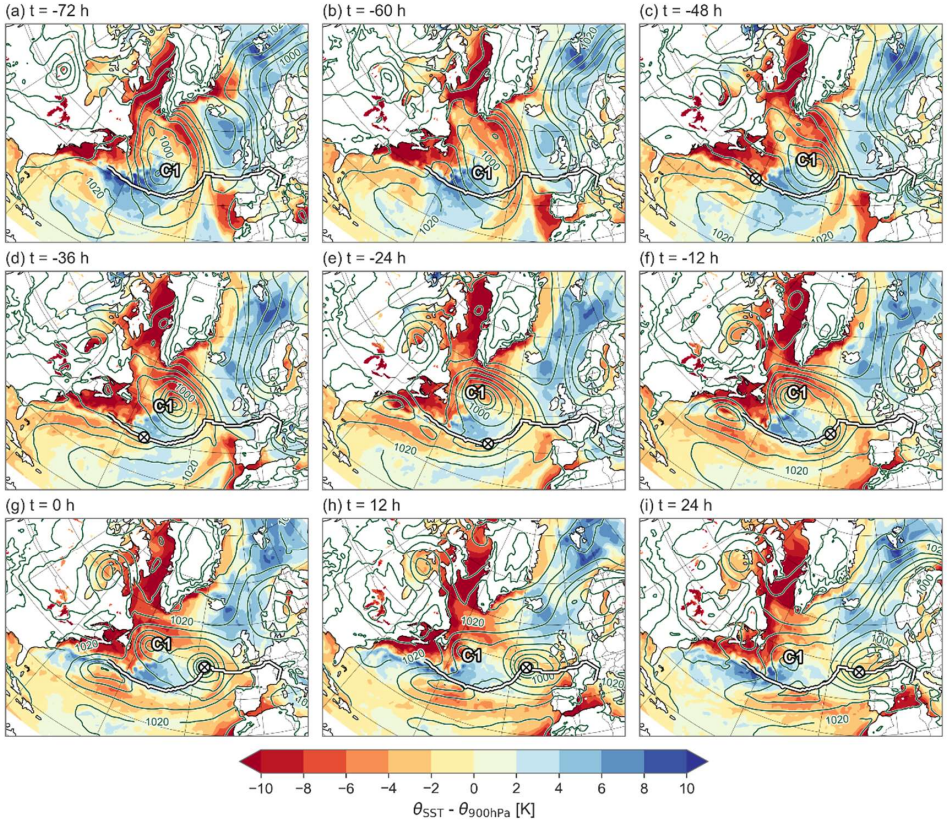

Figure 3: Sea-air potential temperature difference ($\theta_{SST} - \theta_{900hPa}$, in K) associated with an East Atlantic cyclone, for t = -72 h (4 May 2019, 10:00 UTC) to t = 24 h (8 May 2019, 10:00 UTC) in 12-hourly intervals. Additionally shown are SLP contours (in intervals of 5 hPa; dark green lines), the cyclone track (white line), and the cyclone center location (white cross; visible only from -48 hours onward, as cyclogenesis did not occur until -59 hours). Label C1 represents the location of the preceding primary cyclone.

https://doi.org/10.5194/egusphere-2025-1752
Preprint. Discussion started: 25 April 2025

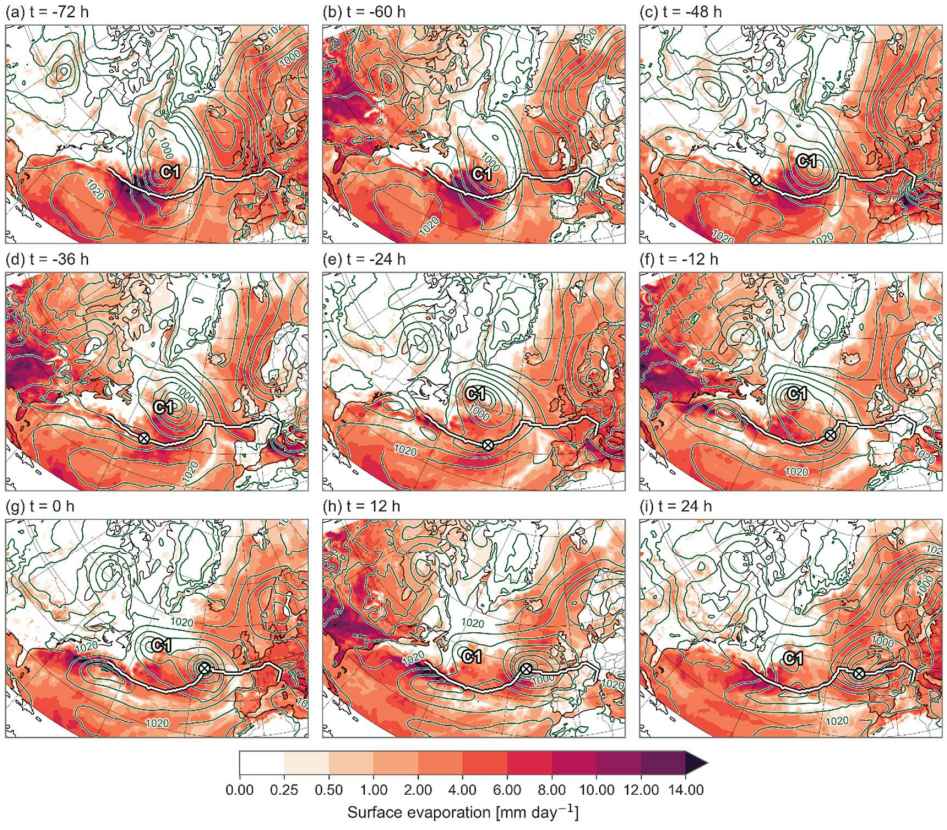

Figure 4: Surface evaporation (in mm day^{-1}) associated with an East Atlantic cyclone, for t = -72 h (4 May 2019, 10:00 UTC) to t = 24 h (8 May 2019, 10:00 UTC) in 12-hourly intervals. Additionally shown are SLP contours (in intervals of 5 hPa; dark green lines), the cyclone track (white line), and the cyclone center location (white cross; visible only from -48 hours onward, as cyclogenesis did not occur until -59 hours). Label C1 represents the location of the preceding primary cyclone.

3.2 Moisture sources and transport pathways

The dynamical flow environment set up by the primary cyclone facilitated significant moisture accumulation in the boundary layer ahead of the developing secondary cyclone up until the cyclone reached its maximum depth. This coincides with the time evolution of precipitation intensity, which peaked during the intensification phase, 12 hours before the cyclone reached its maximum depth (not shown). In the hours after achieving maximum depth, the amount of precipitation notably decreased.

The corresponding moisture sources of the precipitation falling at three distinct times during the cyclone life cycle – the intensification phase (t = -24 h), the mature stage (t = 0 h), and the decay phase (t = 24 h) – are shown in Fig. 5. For this particular cyclone, the largest amount of moisture is taken up by the later precipitating air parcels during the intensification phase (Fig. 5a), on the warm side of the Gulf Stream Front, and only very few uptakes take place over land. As the cyclone

https://doi.org/10.5194/egusphere-2025-1752
Preprint. Discussion started: 25 April 2025

moves eastward throughout its life cycle, the sources of moisture also move eastward (Fig. 5b, c), while most of the uptakes remain along the north-eastward extension of the Gulf Stream Front. The overall moisture source footprint of this cyclone is also reduced over its life cycle, but this is because there is simply less precipitation falling during the later part of its life cycle that can be attributed to a specific source.

The uptake locations observed in Fig. 5 correspond to the regions with high surface evaporation and can be attributed to a combination of flow along the Gulf Stream Front and cold-air advection in the cold sector of a preceding cyclone. The former implies long-range transport, while the latter is a more local process linked to the primary cyclone. The long-range moisture transport is most pronounced during the intensification phase, during which the weighted mean source distance exceeds 2000 km (Fig. 5a). During the time of maximum depth and during the decay, the moisture sources are closer to the cyclone, because the secondary cyclone can quickly access the accumulated moisture ahead of its own location due to its high propagation speed. However, the weighted mean source distance remains above 1500 km (Fig. 5b, c), indicating that long-range moisture transport persists throughout the cyclone's lifecycle.

Throughout most of its life cycle, more than 85% of the moisture content of the precipitating trajectories for this cyclone have, on average, been assigned to a source region, either within the boundary layer or in the free troposphere (Fig. 5). The majority of the moisture is taken up within the boundary layer, implying that most of the moisture is gained by surface evaporation. Roughly 10% of the precipitating air parcels even reach more than 90% attribution, while only 5% have 10% or less attribution, meaning that WaterSip effectively attributes the majority of precipitation for this particular case to its source region. Moisture can also enter air parcels through subgrid-scale convective ventilation or evaporation of precipitation in the free troposphere, but the fraction of moisture uptake identified in the free troposphere is less than 30% in more than 70% of the trajectories.

Figure 5 presents the moisture sources for this case, but does not provide insight into the movement of air parcels before they gained the moisture or their subsequent transport while carrying it. Specifically, if the moisture uptake is already accounted for in the first day(s), Fig. 5 does not reveal where the air parcels were located in the days before uptake, nor whether the moisture was acquired in a single event or multiple stages. To address this, we consider the trajectories of the precipitating air parcels and show their evolution 8-days backward in time on a latitude-longitude grid (Fig. 6a-c) and in the vertical direction (Fig. 6d-f; the 20% of trajectories exhibiting the most intense precipitation). While the moisture source footprint showed a rather coherent source region, the trajectory figures illustrate that there are actually several different pathways how the precipitating air parcels reach the cyclone center.

During the intensification phase, the existence of multiple transport pathways can be identified (Fig. 6a). Many air parcels originated from hotspots of ocean evaporation in the Gulf Stream region, where they were lifted by convection into the mid-troposphere, transported to the cyclone center, and precipitated after converging at the surface and ascending thereafter. Because of the high moisture content of these air parcels, these trajectories experience precipitation in the hours before the cyclone center is reached. Another noteworthy proportion of the precipitating waters arrived from the north of the cyclone, having been embedded in the cyclonic flow of the primary cyclone. These parcels experienced intermittent precipitation, remained aloft, and later descended behind the primary cyclone's cold front. Upon descending into the boundary layer, they

https://doi.org/10.5194/egusphere-2025-1752
Preprint. Discussion started: 25 April 2025

gained substantial moisture, which was then fed into the secondary cyclone. Moreover, there are also some trajectories that travelled over land, where there were several alternating cycles of precipitation and evaporation. Overall, in the days preceding the precipitation, the air parcels were distributed widely throughout the atmosphere (Fig. 6d). The majority of air parcels were concentrated in the mid-troposphere, along with a notable presence of trajectories in the upper-troposphere and near the surface. Gradually, all particles converged at the surface, where they underwent a rapid ascent, shortly before the onset of precipitation. At the time of maximum depth, the pathways of precipitating waters became more uniform (Fig. 6b). Air parcels no longer originated in the Gulf Stream region but instead came from the primary cyclone or further north along the Greenland coast. During the observed pathway, minimal or negligible changes in specific humidity are evident, with the exception of moisture uptakes closer to the cyclone center, suggesting the possibility of the airmasses being initially cold and dry. The trajectories are concentrated slightly closer to the surface compared to the intensification phase, yet some pathways continue to originate from the upper troposphere, indicating substantial descending motion (Fig. 6e).

During the decay phase, there are still trajectories that have a history in being embedded in the cyclonic flow of the primary cyclone (Fig. 6c). However, the number of trajectories originating from the upper layers of the atmosphere has decreased, suggesting that these trajectories most likely have not rained out in the primary cyclone. Instead, the trajectories remained close to the surface (Fig. 6f), where they were able to gain moisture. Furthermore, there are even several trajectories that are embedded in the cyclonic flow of the cyclone itself, as the cyclones becomes more stationary. This is associated with several cycles of precipitation and evaporation, implying that local moisture recycling is becoming important later on in the cyclone life cycle.

This case study demonstrates that moisture sources correspond to regions of high ocean evaporation, but the mechanisms driving moisture uptakes contributing to precipitating waters in the cyclone vary throughout the cyclone's life cycle. Flow along the Gulf Stream Front facilitates long-range moisture transport from warm ocean surfaces, particularly during the intensification phase. Meanwhile, cold-air advection in the cold sectors of either the primary or secondary cyclone is essential throughout the entire life cycle. Two distinct transport pathways emerged for precipitating waters embedded in the cyclonic flow of the primary cyclone: dry air descending from the upper troposphere and cold-air advection along the surface. Both pathways involve strong ascent before precipitation occurs, underscoring the dynamic interplay between moisture sources and transport processes in the development of the secondary cyclone.

https://doi.org/10.5194/egusphere-2025-1752
Preprint. Discussion started: 25 April 2025

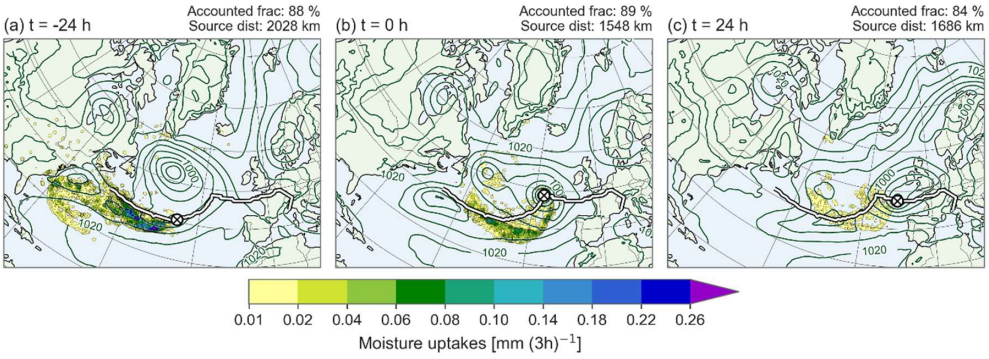

Figure 5: Moisture source footprint of uptakes contributing to precipitation in the cyclone center of an East Atlantic cyclone, for (a) t = -24 h (6 May 2019, 10:00 UTC), (b) t = 0 h (7 May 2019, 10:00 UTC), and (c) t = 24 h (8 May 2019, 10:00 UTC). Additionally shown are MSLP (in intervals of 5 hPa; dark green contours), the cyclone track (white line), and the cyclone center location (white cross). The weighted mean accounted fraction and source distance are given in the top right of each panel.

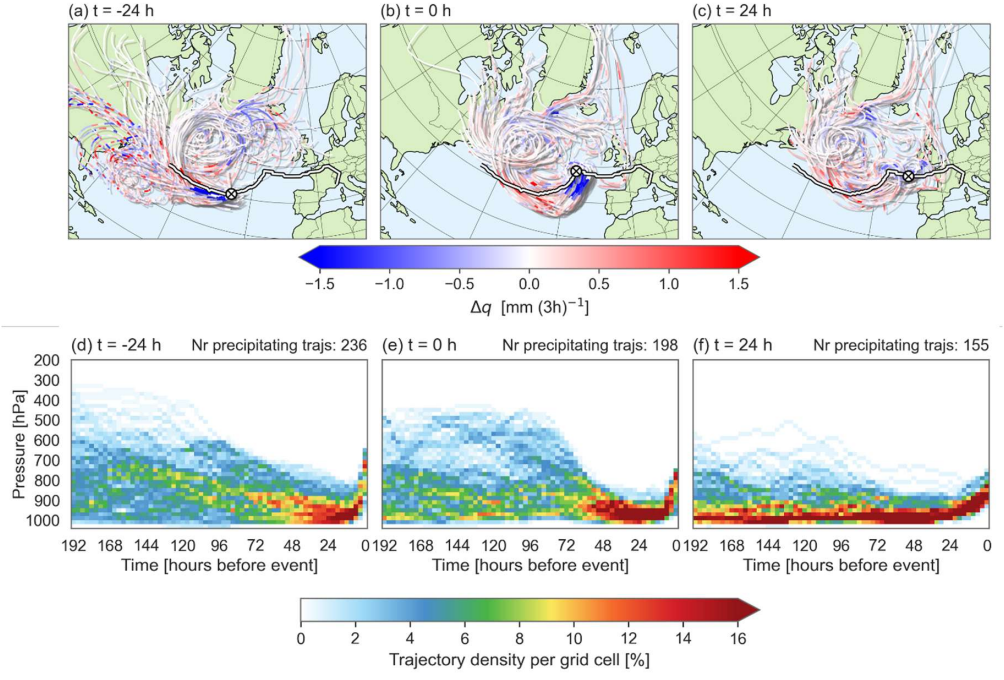

Figure 6: 8-day backward trajectories of the precipitating waters of an East Atlantic cyclone, for (a) t = -24 h (6 May 2019, 10:00 UTC), (b) t = 0 h (7 May 2019, 10:00 UTC), and (c) t = 24 h (8 May 2019, 10:00 UTC). The trajectories are coloured by their change in specific humidity over a 3-hour period (red means moisture uptake events and blue intermittent precipitation). Additionally shown are the cyclone track (white line) and the cyclone center location (white cross). The 20% of trajectories exhibiting the most intense precipitation are mapped on the foreground for the sake of clarity. The three bottom panels show the vertical density of only the most intensely precipitating trajectories, and the number of trajectories shown here is indicated in the top right of each panel.

https://doi.org/10.5194/egusphere-2025-1752
Preprint. Discussion started: 25 April 2025

4. Climatology

In this section, we consider all 688 summertime North Atlantic deep cyclones. We first examine the spatial distribution of the cyclone precipitation, followed by the geographical moisture uptake locations, and a general characterization of the moisture uptake conditions and transport. Finally, we also provide an analysis of the cyclone-relative perspective on the uptake locations and transport pathways. Our goal is to identify common patterns and key moisture source regions, building on insights from the case study.

4.1 Cyclone precipitation

Figure 7 shows the mean spatial distribution of precipitation for the cyclones in each subregion during the intensification phase (t=- 24 h), time of maximum depth (t=0 h) and decay phase (t=24 h). In the figure, the total precipitation from ERA5 is averaged on a cyclone-relative grid, where the grid centre corresponds to the cyclone center, regardless of the geographical location in the study area. For all subregions, precipitation within the cyclone center (black circle) is highest during the intensification phase (Fig. 7a, d, g, j), prior to the cyclones reaching their maximum depth. This indicates that the maximum vertical motion, which ultimately triggers the precipitation, occurs before the minimum MSLP. In contrast, the lowest precipitation rates are observed during the decay phase (Fig. 7c, f, i, l).

Cyclones in the Gulf Stream region exhibit the highest precipitation rates throughout their entire life cycle, while those in the Nordic Seas show the lowest. The relatively cold ocean surface in the Nordic Seas limits surface evaporation and moisture supply, leading to low precipitation rates. In contrast, the Gulf Stream region experiences higher precipitation rates due to enhanced surface evaporation over a warmer ocean surface, which significantly moistens the warmer boundary layer (Aemisegger and Sjolte, 2018; Bui and Spengler, 2021; Pfahl et al., 2014). In addition, the presence of dry air masses associated with subsidence in the downward branch of the Hadley circulation further enhances evaporation by lowering near-surface relative humidity. Together, these processes increase the moisture content in the Gulf Stream region, leading to more convective precipitation and allowing for stronger latent heat release during large-scale ascent within the cyclones, which in turn serves to further intensify them. As a result, the strongest cyclones are observed in the Gulf Stream region (Fig. 1e). In the early phase of the cyclone life cycle, the higher precipitation observed in the Gulf Stream region relative to other subregions is due to stronger convective precipitation (Fig. A2). As the cyclone progresses towards its maximum intensity, there is also a significant increase in large-scale precipitation, peaking just before the time of maximum depth. Even during the decay phase, large-scale precipitation remains higher for Gulf Stream cyclones compared to those in other regions of the North Atlantic.

In addition to these differences in the magnitude, there are also important differences in the spatial distribution of precipitation around the cyclone center across the subregions. In the Gulf Stream region, the highest precipitation rates are concentrated near the cyclone center, displaying a near-symmetrical structure (Fig. 7a-c). This symmetry reflects the influence of cyclones with tropical origins, which have undergone tropical-extratropical transitions and tend to be more intense. In contrast, cyclones in the other subregions exhibit a more typical midlatitude cyclone structure, characterised by precipitation concentrated along

https://doi.org/10.5194/egusphere-2025-1752
Preprint. Discussion started: 25 April 2025

the warm and cold fronts – primarily generated by dynamical uplift – and in the warm sector, associated with thermodynamically driven convection (Fig. 7d-l). A similar cold frontal signature is also evident in Gulf Stream cyclones, though not until later in the decay stage when the cyclone adopts a more extratropical structure.

In the regions not affected by cyclones with tropical origins, a prominent diagonal band of precipitation that stretches from the southwest (-10°, -10°) to the northeast (+5°, +5°) is visible, which is mainly present during the intensification phase and at the time of maximum depth. Within this region, precipitation rates range from 8 to more than 32 mm day^{-1} at the center of the cyclone, suggesting the presence of the WCB. As the cyclones evolve, occluded fronts develop, resulting in a narrowing of the warm sector and an increasing gap between the warm sector and the cyclone's low-pressure center. This transition marks the decay phase, which is accompanied by a significant drop in precipitation at t = 24 h for all cyclones except those in the Gulf Stream region. Although exact occlusion timings are difficult to determine due to the absence of frontal detection and because Fig. 7 is a spatial composite, the observed patterns support this interpretation.

In summary, precipitation associated with North Atlantic deep cyclones depends on cyclone strength and moisture availability. Precipitation rates therefore peak during the intensification phase when vertical motions are strongest, and in the Gulf Stream region, where there is abundant moisture from strong ocean evaporation over warm waters.

https://doi.org/10.5194/egusphere-2025-1752
Preprint. Discussion started: 25 April 2025

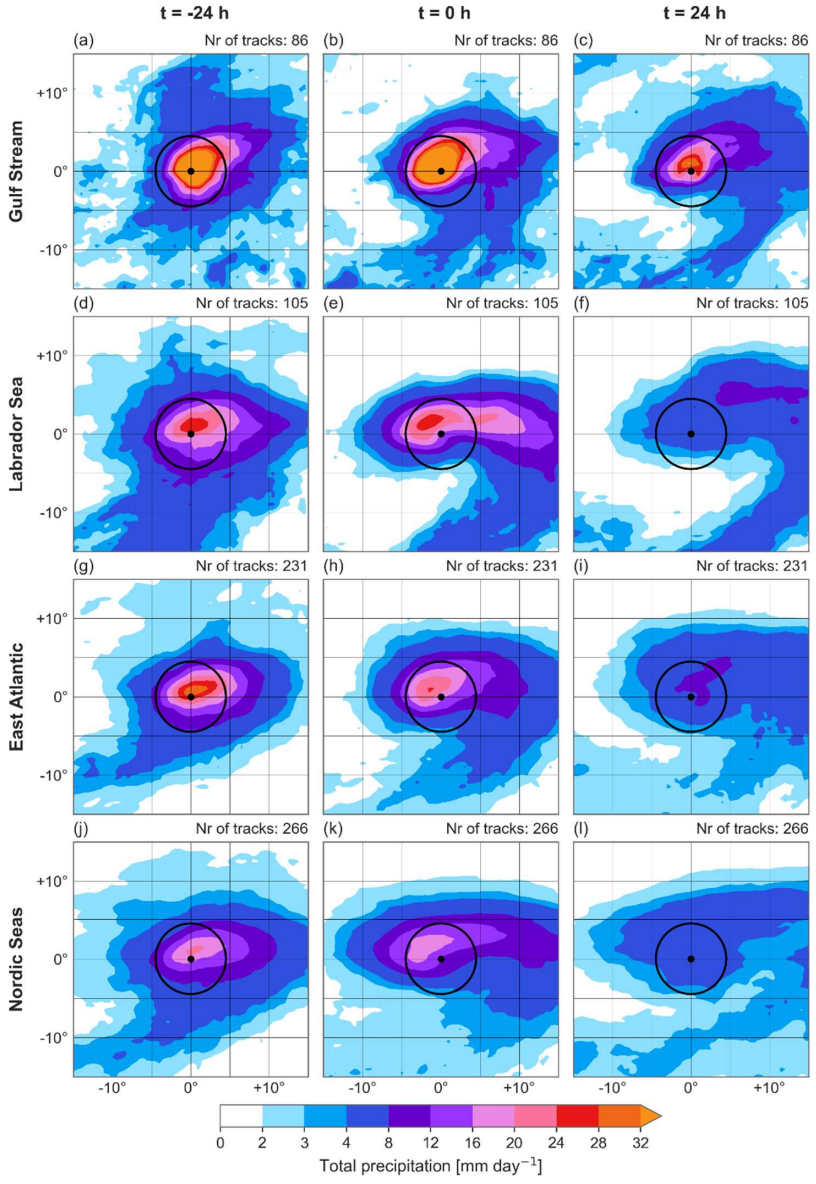

Figure 7: Cyclone-relative composites of the mean total precipitation (in mm day^{-1}) of the cyclones in (a)-(c) the Gulf Stream, (d)-(f) the Labrador Sea, (g)-(i) the East Atlantic, and (j)-(l) in the Nordic Seas from t = -24 h to t = 24 h in intervals of 24 h. Precipitation is averaged over 12-hourly intervals centered on the given relative time t. Additionally shown are the cyclone center location (black dot) and surrounding circle with a radius of 500 km (black circle). The number of cyclones contributing to the composite is indicated in the top right of each panel.

https://doi.org/10.5194/egusphere-2025-1752
Preprint. Discussion started: 25 April 2025

4.2 Geographical origin of moisture

The geographical locations of moisture uptake associated with precipitation falling during the three phases of the cyclone life cycle, for the four subregions, are shown in Fig. 8. Overall, WaterSip effectively attributes the majority of precipitation to its source region. For approximately 90% of all precipitating waters, over 50% of the initial moisture could be accounted for within the 8-day period (Fig. A3). The remaining moisture either originates from an unidentified source region or was acquired by air parcels beyond the backward trajectory tracking period.

Figure 8 highlights a clear pattern: cyclones attaining their maximum depth in the Gulf Stream region take up the most moisture, while those in the Nordic Seas acquire the least. This finding is consistent with what we found for precipitation (Fig. 7). Moreover, moisture uptake associated with precipitation from cyclones in all subregions is pronounced in the western part of the North Atlantic, and concentrated on the warm side of the Gulf Stream Front. These areas provide exceptional moisture supply due to strong oceanic evaporation over elevated sea surface temperatures. This pattern is important because it applies to all subregions within the North Atlantic, making it a consistent and robust feature of moisture sources for cyclone precipitation. The findings are also in agreement with a previous study (Pfahl et al., 2014) of moisture sources for WCBs and underline the significance of these sources.

An intriguing detail of the moisture source footprint for cyclones in the Gulf Stream region and East Atlantic is its slight extension to the southeast, which likely reflects the influence of cyclones with tropical origins. These cyclones contribute to the moisture supply by transporting moisture from the subtropics to the extratropics. However, this southeastern extension is not the primary source of moisture and does not reach deep into the tropics, as the tropical air masses already have a high moisture content upon arriving in the region, thereby limiting further evaporation from the ocean surface.

Throughout the cyclone's life cycle, there is a slight shift towards the east in moisture sources. However, this shift is only evident for cyclones in the East Atlantic and Nordic Seas regions, where the moisture sources have moved along the northeastern extension of the Gulf Stream Front.

In addition, the large spatial extent of the moisture source footprint associated with cyclone precipitation is striking, especially during the intensification phase. This suggests that the moisture contributing to these cyclones often comes from remote sources. Essentially, North Atlantic cyclones do not depend solely on local moisture; they access moisture reservoirs distributed across large parts of the ocean, thereby increasing their moisture supply. Local moisture recycling becomes more important when the cyclones start to decay, but during this phase moisture uptake is lower.

Lastly, it is observed that there are also some continental moisture sources for cyclone precipitation associated with cyclones in the Labrador Sea and, to a lesser extent, the East Atlantic during the summer months. This finding suggests that land evapotranspiration becomes a significant contributor to cyclone precipitation during the summer season (Pfahl et al., 2014; van der Ent and Tuinenburg, 2017). The extent to which surface evapotranspiration contributes to cyclone precipitation depends on soil moisture availability, but a discussion of this influence and variability is beyond the scope of this research. Nevertheless, this finding underscores the diverse nature of the origin of moisture precipitating in summertime cyclones,

https://doi.org/10.5194/egusphere-2025-1752
Preprint. Discussion started: 25 April 2025

emphasizing the significance of taking into account seasonal variability and terrestrial impacts in the cyclone related water cycle.

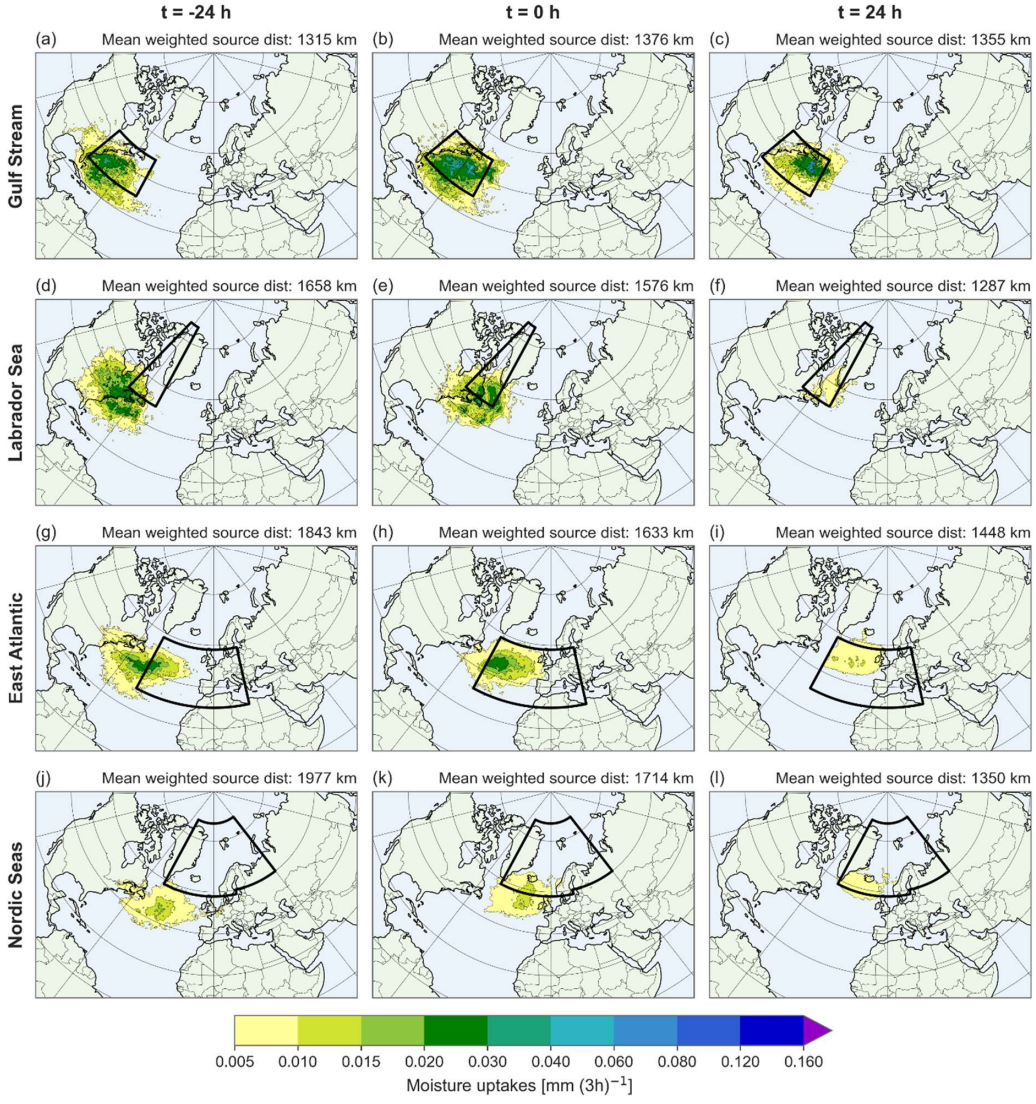

485

Figure 8: Climatological mean moisture source footprint of moisture uptakes contributing to precipitation in the cyclone center of the cyclones in (a)-(c) the Gulf Stream, (d)-(f) the Labrador Sea, (g)-(i) the East Atlantic, and (j)-(l) in the Nordic Seas from t = -24 h to t = 24 h in intervals of 24 h. The regions used for the selection of the cyclones at their time of maximum depth are outlined by black boxes and the mean weighted source distance is given in the top right of each panel.

https://doi.org/10.5194/egusphere-2025-1752
Preprint. Discussion started: 25 April 2025

4.3 Moisture uptake characteristics

Figure 9 provides insight into the environment in which the moisture uptakes take place. Unlike Fig. 8, which focuses on three specific phases during the cyclone life cycle, Fig. 9 presents data at 3-hourly intervals, allowing us to analyse how these characteristics evolve over time.

Moisture uptake occurs over a wide range of distances from the cyclone center, from local sources to over 3000 km away from the location where the precipitation ultimately falls. Throughout the cyclone life cycle, about 20% of the moisture comes from sources within 1000 km, a fraction that remains relatively constant. However, moisture uptake from sources within 500 km is remarkably rare. During the intensification phase of the cyclone, roughly 20% of the moisture sources are located more than 2500 km from the cyclone center, indicating enhanced long-range transport during this phase. This finding is consistent with Fig. 8, which highlighted that the moisture source footprints have a large spatial extent, especially during the intensification phase. While distant moisture sources are still observed, the contribution of moisture originating 1000-1500 km from the precipitation locations increases from just over 20% to nearly 40% during the decay phase.

Most of the moisture uptake occurs over the ocean surface (Figs. 8 and 9c), where near-surface temperatures are between 280-290 K for 50% of the uptake locations (Fig. 9b). During the intensification phase, 20% of the moisture uptakes occur in environments with near-surface temperatures above 290 K. These warm temperatures are characteristic of the air masses that traverse the Gulf Stream Front or originate from the subtropics, and they are most pronounced in the Gulf Stream cyclones (Fig. A4). As the cyclone progresses, the contribution of moisture uptake from colder air masses ($\leq$ 285 K) increases from 30% to over 50% at the expense of moisture uptake in warmer air masses, which aligns with the poleward propagation of the cyclones.

While contributions from land surfaces are significant, they are generally secondary to oceanic moisture sources. For at least 80% of the cyclones, less than 50% of the moisture comes from land. However, land sources play a dominant role for cyclones intensifying in the Labrador Sea, where over 60% of cyclones receive more than half of their moisture from land during this phase (Fig. A5). In fact, for 25% of cyclones in this subregion, moisture originating from land remains the primary contributor until they reach their maximum depth, with over 70% of the precipitating waters linked to terrestrial sources.

The atmospheric residence time – the time between moisture uptake and precipitation – is shown in Fig. 9d. More than 80% of the moisture uptake occurs within four days of precipitation, suggesting that this is the typical residence time for cyclone-related moisture during the summer. For the remainder, nearly 15% of the moisture rains out within only two days, indicating that there is also a rapid turnover within the cyclone system. Despite the greater source distances observed during the intensification phase (Fig. 9a), the residence time remains relatively constant, suggesting that moisture must be transported more rapidly during this phase. This is consistent with the presence of stronger winds that facilitate faster long-range transport. As the cyclone matures, weaker winds tend to slow down the convergence of moisture at the surface, but at the same time the source distances are not as large.

https://doi.org/10.5194/egusphere-2025-1752
Preprint. Discussion started: 25 April 2025

The analysis reveals that summertime deep cyclones in the North Atlantic exhibit subtle shifts in their moisture uptake characteristics. During the intensification phase, stronger winds enhance long-range transport, allowing moisture to originate from distances exceeding 2500 km. These sources are typically linked to land evapotranspiration or evaporation from warm ocean surfaces into subtropical air masses. As the cyclone progresses, these contributions decrease, and moisture uptakes from sources 1000–1500 km away become increasingly important. At most of these locations, near-surface temperatures are between 275-285 K, hinting at cold-air advection.

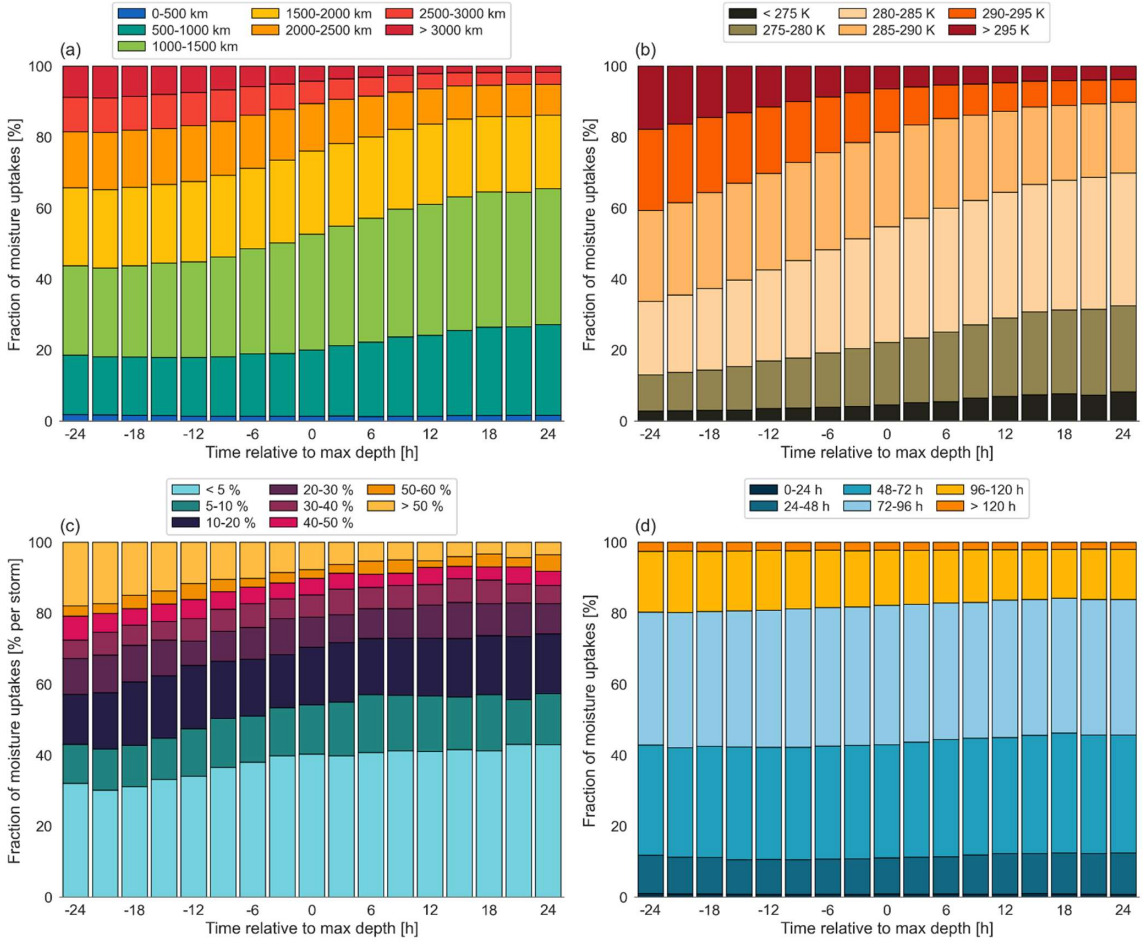

Figure 9: Characteristics of moisture uptakes contributing to precipitation at t = -24 h to t = 24 h in 3-hourly intervals, associated with cyclones from all regions. Shown are uptake contributions according to (a) distance between uptake and precipitation locations, (b) 2 meter temperature, (c) fraction of uptakes that have occurred over land, and (d) moisture residence time.

https://doi.org/10.5194/egusphere-2025-1752
Preprint. Discussion started: 25 April 2025

4.4 Vertical distribution of the precipitating waters

Further insight into how the moisture is transported to the cyclone center can be obtained by analysing the vertical distribution of the trajectories of precipitating air parcels. Figure 10 shows the vertical density of these trajectories over the full eight-day period preceding precipitation. Since the figure represents the mean of all precipitating trajectories across 688 cyclones, it is difficult to identify distinct vertical transport pathways. However, some common patterns emerge.

During all three phases in the cyclone life cycle, air parcels are concentrated in the lower troposphere (below 800 hPa) in the days leading up to precipitation, followed by a pronounced ascending motion within the last 12 hours before the precipitation. This ascent primarily takes place in the warm sector of the cyclone, where strong latent heat release further enhances vertical motion. The accumulation of moisture near the cyclone center is followed by lifting within the WCB until the air cools and reaches saturation.

Previous studies (e.g., Madonna et al., 2014) have identified WCBs by selecting trajectories that ascend at least 600 hPa within 48 hours. While we did not explicitly isolate WCB trajectories in our analysis, a visual inspection of Fig. 10 reveals that the trajectories do not reach altitudes above 500 hPa. This observation suggests that ascent of 600 hPa or more does not occur, implying that vertical motions in the WCB of summertime deep North Atlantic cyclones are weaker than those observed in other seasons. This likely results from reduced baroclinicity and overall weaker cyclones in summer, leading to less intense ascent within the WCB.

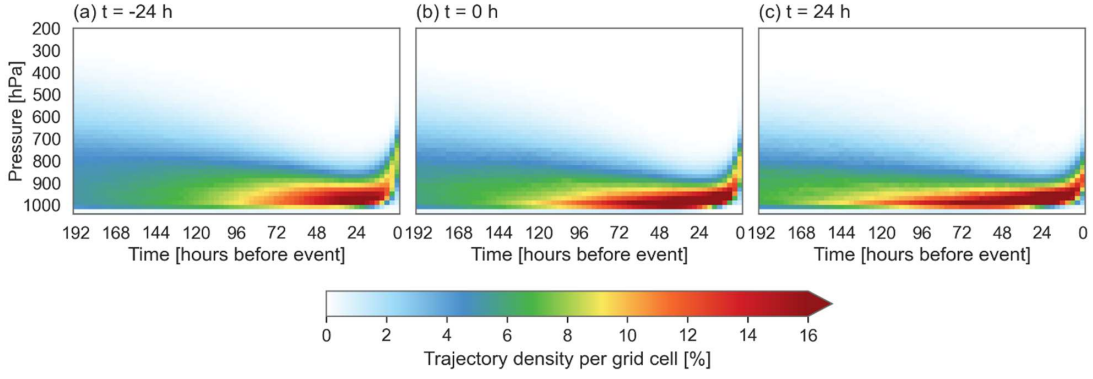

Figure 10: The mean vertical density of only the 20% of trajectories of each cyclone exhibiting the most intense precipitation, for (a) t = -24 h, (b) t = 0 h, and (c) t = 24 h.

4.5 Cyclone relative perspective on moisture uptake

Based on our previous findings, we have identified that moisture from the warm side of the Gulf Stream Front is supplied to the cyclone centers in the North Atlantic. From a cyclone-relative perspective, these moisture sources lie to the south of the cyclones. Additionally, we observed that cold-air advection can contribute to boundary-layer moistening. To quantify this for

https://doi.org/10.5194/egusphere-2025-1752
Preprint. Discussion started: 25 April 2025

the entire cyclone subset and to better understand where it occurs relative to cyclone centers, we study the spatial distribution of surface evaporation within and around the cyclone center. The moisture source footprints produced by WaterSip are aggregated fields over the 8-day period, making it impossible to examine instantaneous moisture uptake locations and their positioning relative to the cyclone center. Nevertheless, composites of surface evaporation for the days prior and during cyclone development can be examined. Figure 11 shows the mean surface evaporation and sea level pressure for the cyclones in all subregions on a cyclone-relative grid in 12-hourly intervals. Please note that evaporation during this period does not necessarily contribute directly to precipitation in the developing cyclones.

In the early phase of cyclone development, the MSLP contours indicate a distinct anticyclone to the southeast of the cyclone center, as was observed in the case study. Surface evaporation is particularly high within and to the south of this anticyclone, as warm, subsaturated air subsides over the warm ocean surface, promoting enhanced evaporation (Boutle et al., 2010). Taking into account the findings of Okajima et al. (2024), which suggest a net moisture transport from anticyclonic to cyclonic systems, it is plausible that moisture evaporating in this region contributes, at least to some extent, to precipitation in the developing cyclone. Over time, evaporation rates in this region decline.

Closer to the cyclone center, strong surface evaporation is also evident. One pronounced region of elevated evaporation appears southwest of the developing cyclone, co-located with the cyclone's cold sector. Here, cold, dry air descends behind the cold front, creating a sharp temperature contrast with the ocean surface and facilitating strong upward latent heat fluxes. According to Boutle et al. (2010), horizontal divergence induced by boundary-layer drag transports the moisture away from this region, maintaining the saturation deficit in the cold sector. However, it is unlikely that the moisture evaporating behind the cold front is transported to the warm sector or into the WCB, as the strong horizontal divergence and subsidence in the cold sector act as barriers to vertical ascent and transport across the front. Instead, much of this moisture rains out further from the cyclone center or remains in the boundary layer and can be utilized by another cyclone, assuming that the subsequent system propagates over the moist boundary layer. This mechanism suggests a potential moisture preconditioning effect, wherein surface evaporation in one cyclone's cold sector influences moisture availability for subsequent cyclones following a similar path.

https://doi.org/10.5194/egusphere-2025-1752
Preprint. Discussion started: 25 April 2025

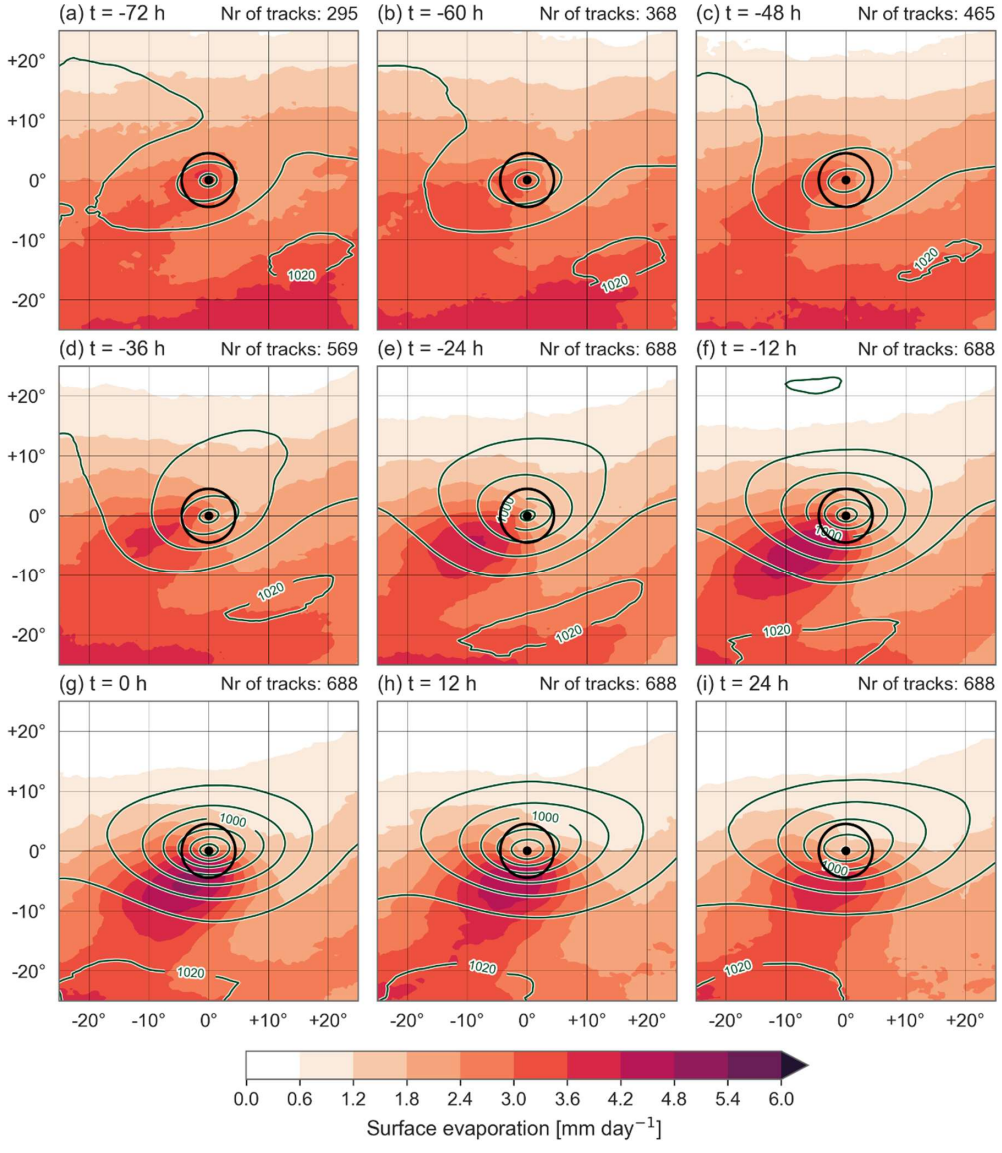

580 **Figure 11: Cyclone-relative composites of the surface evaporation (in mm day^{-1}) of all cyclones in the North Atlantic, for t = -72 h to t = 24 h in 12-hourly intervals. Surface evaporation is averaged over 12-hourly intervals centered on the given relative time t. Additionally shown are MSLP (in intervals of 5 hPa; dark green contours), the cyclone center location (black dot), and surrounding circle with a radius of 500 km (black circle). The number of cyclones contributing to the composite is indicated in the top right of each panel.**

https://doi.org/10.5194/egusphere-2025-1752
Preprint. Discussion started: 25 April 2025

5 Conclusions

5.1 Synthesis

In this study, we have analysed summertime extratropical cyclones, since they have received less attention than their winter counterparts, leaving key aspects of the cyclone-related water cycle poorly understood. To address this gap, we studied the precipitation distribution and identified precipitating waters within 500 km from the cyclone center for both a case study of a representative cyclone and a climatology of 688 deep summertime cyclones. By computing backward trajectories and analysing changes in specific humidity along these trajectories, we were able to pinpoint the moisture sources, characterize the uptake environment and understand moisture transport pathways. Below, answers per research question are given.

Q1: What is the spatial distribution of precipitation within and around the cyclone center?

The bulk of the precipitation associated with summertime cyclones falls close to the cyclone center within the WCB, mainly during the intensification phase. This precipitation is driven by vertical motions, frontogenetic dynamics and thermodynamic (local) convection. Moreover, cyclones in the Gulf Stream region exhibit the highest precipitation rates throughout their entire life cycle. This can be attributed to higher surface evaporation over a relatively warmer ocean surface in this region, which significantly moistens the boundary layer and supplies the cyclones with more moisture than in the other subregions.

Q2: What are the geographical and cyclone-relative moisture sources of the precipitating waters?

From a geographical perspective, three moisture source regions are identified: (1) the warm side of the Gulf Stream Front, where evaporation from the ocean surface is particularly strong; (2) continental sources, which are especially relevant for cyclones in the Labrador Sea; and (3) a southeastward extension of the moisture source footprint into the subtropics, likely reflecting the influence of cyclones with tropical origins that are present in the East Atlantic and Gulf Stream region. Another region of high surface evaporation, though not necessarily contributing to the precipitation in the cyclone center itself, is within the cold sector of the cyclone. From a cyclone-relative perspective, this region is located to the southwest of the cyclone center. Here, significant moisture accumulates within the boundary and is transported away by horizontal divergence where it eventually rains out further from the cyclone center or remains in the boundary layer. In the latter case, the moisture could potentially supply another cyclone that propagates through the region. Our case study confirms this process, showing clear evidence of moisture being handed over from one cyclone to the next.

Q3: In which dynamical environment do moisture uptakes take place?

Moisture uptake occurs through two main mechanisms over the ocean. First, there is flow across the Gulf Stream Front, where the strong SST gradient induces intense ocean evaporation. This occurs in regions where near-surface temperatures exceed 290 K, and the sea-air potential temperature difference is positive but situated near a sharp transition to negative values. Second, moisture uptake occurs in regions of cold-air advection, such as the cold sector of a cyclone. In these environments,

https://doi.org/10.5194/egusphere-2025-1752
Preprint. Discussion started: 25 April 2025

near-surface temperatures are lower (below 280 K), but the underlying ocean remains relatively warm, creating a strong temperature contrast that drives intense upward latent heat fluxes. In addition to these oceanic sources, continental moisture uptake also plays an important role in summer, when land evapotranspiration contributes to cyclone-related precipitation.

Q4: How do the uptake and moisture transport characteristics change throughout the life cycle of a cyclone?

During the early stages of cyclone development, moisture is delivered to the cyclone center from more remote sources located on the warm side of the Gulf Stream Front, where the near-surface temperature can exceed 290 K. The moist and warm air masses have undergone convective ascent and are transported in the mid-troposphere before reaching the cyclone. Meanwhile, moisture uptakes associated with cold-air advection are responsible for cyclone precipitation throughout the entire life cycle. As revealed by the case study, this occurs when cold air masses from the north move equatorward along the surface and interact with the ocean, or when dry air masses descend behind the cold front of either the primary or secondary cyclone. These moisture sources, located closer to the cyclone center, become more dominant as cyclones generate less precipitation and start to decay. Consequently, the source distances are highest during the intensification phase and decrease throughout the cyclone life cycle. Despite this shift in source regions, the atmospheric residence time of moisture remains relatively constant, at about four days.

5.2 Discussion and final thoughts

Previous studies, such as Papritz et al. (2021), have extensively analysed moisture sources and uptake characteristics for North Atlantic deep cyclones in winter. During this season, the stronger equator-to-pole temperature gradient intensifies the jet stream, resulting in cyclones with higher wind speeds and more intense vertical motions within the WCB. According to Papritz et al. (2021), cyclone-related precipitation in winter is mainly fuelled by strong ocean evaporation, especially when cold air is advected over a relatively warm ocean surface. In summer, however, the atmosphere is warmer, reducing the temperature contrast that drives strong evaporation. In addition, cyclones develop in a weaker baroclinic environment (Chang and Song, 2006). Nevertheless, evaporation over very warm SSTs can still provide substantial moisture to the warmer summer atmosphere, resulting in high specific humidity values. These seasonal differences motivated us to study how the cyclone-related water cycle is shaped in summer.

Regarding the moisture sources of the precipitating waters, we found that the Gulf Stream region and the Gulf Stream Front serve as robust moisture sources in both summer and winter, underscoring their importance. However, despite this and other similarities, there are also notable seasonal differences in moisture sources and transport pathways. In summer, for example, subtropical moisture plays a more prominent role, especially during the intensification phase, leading to more long-range moisture transport into the storm system. In contrast, winter cyclones tend to rely more on local moisture sources, with a higher contribution from short-distance evaporation regions. The mean atmospheric residence time of moisture is also longer in summer, averaging about four days compared to three days in winter (Papritz et al., 2021; van der Ent and Tuinenburg, 2017). This extended residence time is likely the result of weaker atmospheric moisture convergence, reduced cyclone strength, and

https://doi.org/10.5194/egusphere-2025-1752
Preprint. Discussion started: 25 April 2025

the increased water vapor holding capacity of a warmer atmosphere, which delays saturation. In addition, continental moisture sources become more relevant in summer, especially for cyclones developing in the Labrador Sea.

Another seasonal distinction is the role of cyclone clusters in moisture transport. In winter, moisture sources are often associated with a preceding cyclone, with moisture uptake occurring within the cold sector of the primary cyclone or within the interaction zone between the cyclone and an anticyclone (Papritz et al., 2021). In our analysis for summer, we presented a case study that illustrates that such cyclone clusters also occur in summer. In the composites of all 688 cyclones, however, we could not identify a clear feeder air stream transporting moisture from the primary cyclone to the northeast into the developing cyclone, despite the presence of an anticyclone. This suggest that there are fewer cyclone clusters in our subset. This is in agreement with Weijenborg and Spengler (2024), who found that cyclone clusters are less common in summer compared to winter.

Weijenborg and Spengler (2024) distinguish two types of cyclone clusters: a 'Bjerknes' type and a stagnant type. The former is in line with the original idea of Bjerknes and Solberg (1922), where several successive cyclones follow a similar path. These systems are more common in winter and are more likely to appear in composite analyses. The latter, stagnant cyclone clusters, remain nearly stationary throughout their life cycle. Consequently, our inability to detect a preceding cyclone in the summer composite (Fig. 11) may be due to both the reduced frequency of 'Bjerknes' cyclone clusters and the difficulty of compositing stagnant systems due to inconsistent relative positioning between cyclones. Future research could address this by distinguishing between primary, secondary, or individual cyclones, and analysing the cyclone-related water cycle for each group separately. A methodology for this is proposed by Priestley et al. (2017, 2020), which applies a frontal identification algorithm and checks whether detected cyclones form along the trailing cold front of a previous cyclone.

Once moisture reaches the cyclone center, it contributes to precipitation through convergence at the surface and subsequent ascending motions in the warm sector and within the WCB. These processes are similar in both summer and winter cyclones, but the strength of vertical motions and the role of moisture availability differ. In winter, stronger baroclinicity enhances vertical ascent in the WCB, lifting the moisture all the way into the free troposphere. In contrast, our analysis shows that the air parcels responsible for precipitation in the 688 summer cyclones cover less vertical distance, as weaker baroclinicity results in reduced vertical uplift within the WCB. However, increased moisture inflow, driven by the Clausius-Clapeyron relationship, compensates for this by ensuring that even with less uplift, the higher moisture content in warmer air parcels results in similar precipitation once saturation is reached.

In addition to the WCB, identifying other cyclone-related features, such as ARs and fronts, may provide further insight into summer precipitation processes. ARs, in particular, occur more frequently in summer (Knippertz et al., 2018) and may play an important role in supplying moisture to summer cyclones. Similarly, fronts are known to contribute significantly to precipitation in the Northern Hemisphere storm track, with up to 80% of precipitation in these regions being associated with fronts (Catto et al., 2012; Konstali et al., 2024). A systematic approach to identifying these features, such as the methodology proposed by Konstali et al. (2024), would improve our understanding of precipitation generation mechanisms related to summer cyclones.

https://doi.org/10.5194/egusphere-2025-1752
Preprint. Discussion started: 25 April 2025

Both our case study and climatological analysis suggest that moisture uptake occurs in two distinct dynamical environments. The first is flow across the Gulf Stream Front, associated with strong evaporation. The second involves cold-air advection, in which relatively colder air from the north acquires moisture either from the cold sector of a preceding cyclone (a process more common in winter) or from the developing cyclone's own cold sector (which appears to be more important in summer). As for precipitation, the WCB remains a key mechanism, although its intensity is weaker in summer. However, this reduced intensity is offset by an increase in atmospheric moisture transport. These findings highlight not only the seasonal differences in cyclone dynamics but also the necessity of studying summer cyclones to improve our understanding of the global water cycle. Moreover, the poleward shift of the storm track in summer, which increases the frequency of cyclones reaching western and northern Europe (Mesquita et al., 2008), is projected to intensify under climate change. Priestley and Catto (2022) suggest that this shift will extend further into Europe, affecting both summer and winter cyclones. This raises the possibility that future climate conditions may lead to summer-like cyclone behaviour becoming more prevalent throughout the year.

Appendix A

Appendix A consists of additional figures that complement the methodology and results section of this study.

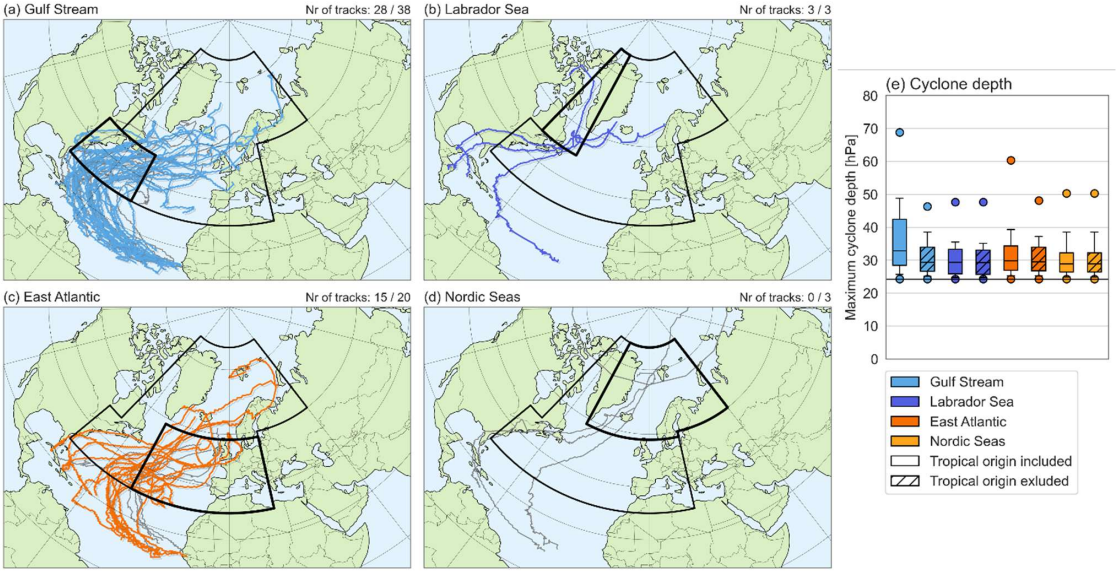

Figure A1: Selected tracks with tropical origin in (a) the Gulf Stream region, (b) the Labrador Sea, (c) the East Atlantic Ocean, and (d) the Nordic Seas. The selected tracks are highlighted in colour and meet the three criteria of duration, intensity and location. At the top right of each panel, the number of cyclone tracks that have been selected are given as the proportion relative to the total of tracks with tropical origin within each of the four subregions. (e) The distribution of the maximum depth of the selected cyclones in the four subregions when the ones with tropical origin are included (final subset; solid boxes) and excluded (hatched boxes). The black horizontal line represents the threshold of the 80th percentile of all tracks. In addition, the whiskers indicate the 10th-90th percentile range, and the dots show maxima and minima.

https://doi.org/10.5194/egusphere-2025-1752
Preprint. Discussion started: 25 April 2025

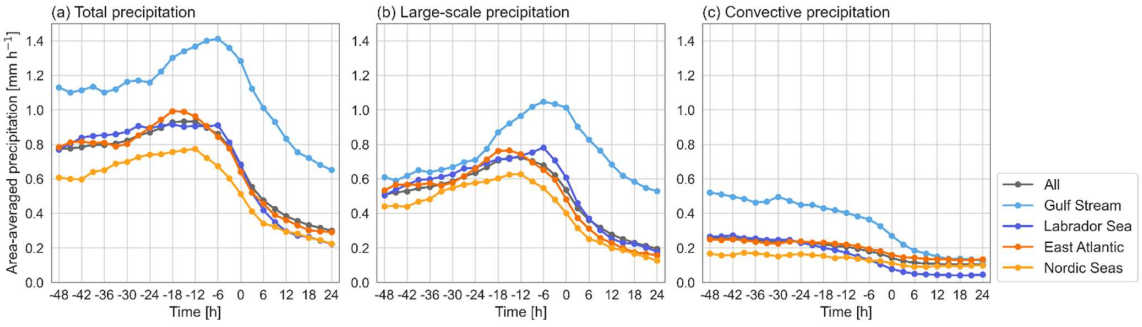

Figure A2: Area-averaged (a) total precipitation, (b) large-scale precipitation, and (c) convective precipitation (all in mm h^{-1}) within the time interval t = −24 hours to t = 24 hours. The grey line is the mean for all tracks. The coloured lines are the means for each subregion.

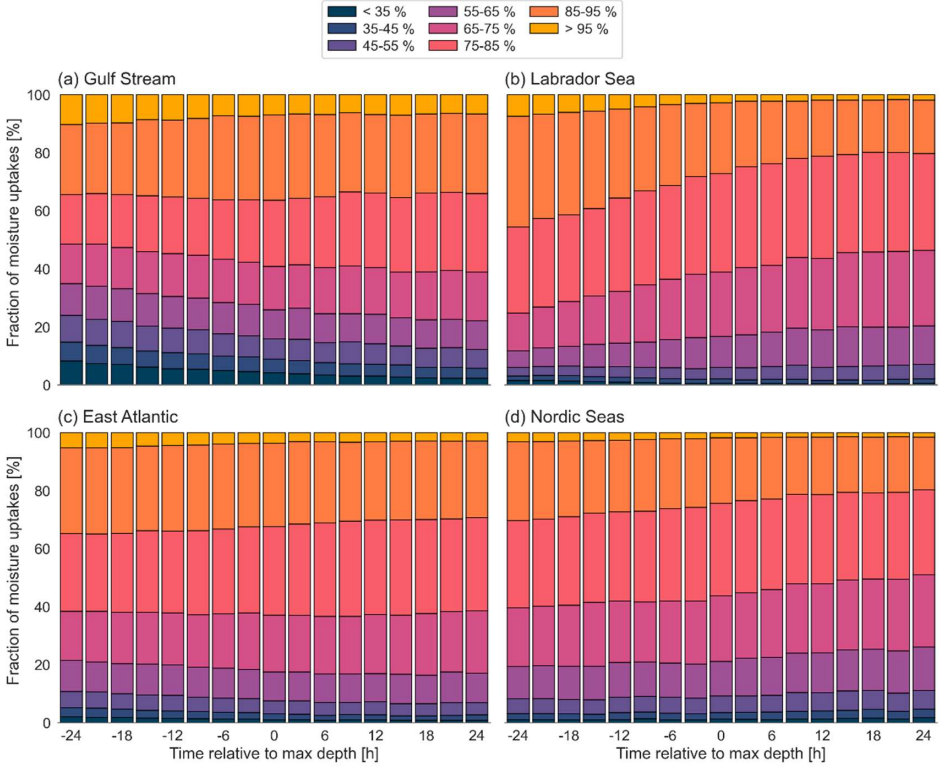

Figure A3: Uptake contributions according to the fraction of precipitation that has been assigned to a source region, at t = -24 h to t = 24 h in 3-hourly intervals, associated with cyclones in (a) the Gulf Stream, (b) the Labrador Sea, (c) the East Atlantic, and (d) in the Nordic Seas.

https://doi.org/10.5194/egusphere-2025-1752
Preprint. Discussion started: 25 April 2025

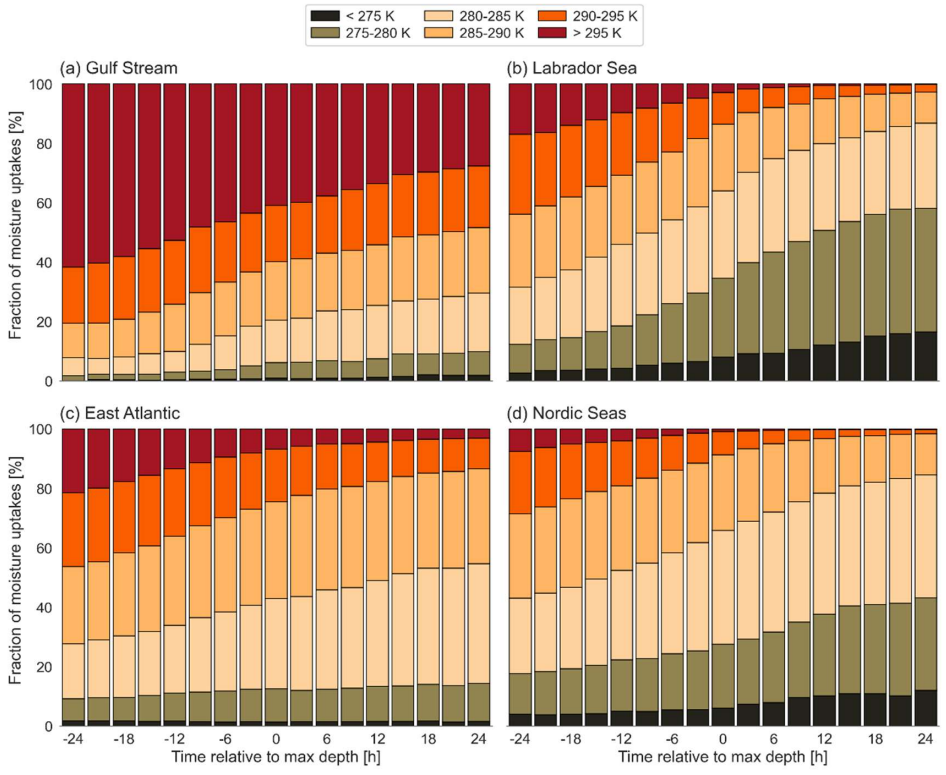

715

Figure A4: Uptake contributions according to the 2 meter temperature, at t = -24 h to t = 24 h in 3-hourly intervals, associated with cyclones in (a) the Gulf Stream, (b) the Labrador Sea, (c) the East Atlantic, and (d) in the Nordic Seas.

https://doi.org/10.5194/egusphere-2025-1752
Preprint. Discussion started: 25 April 2025

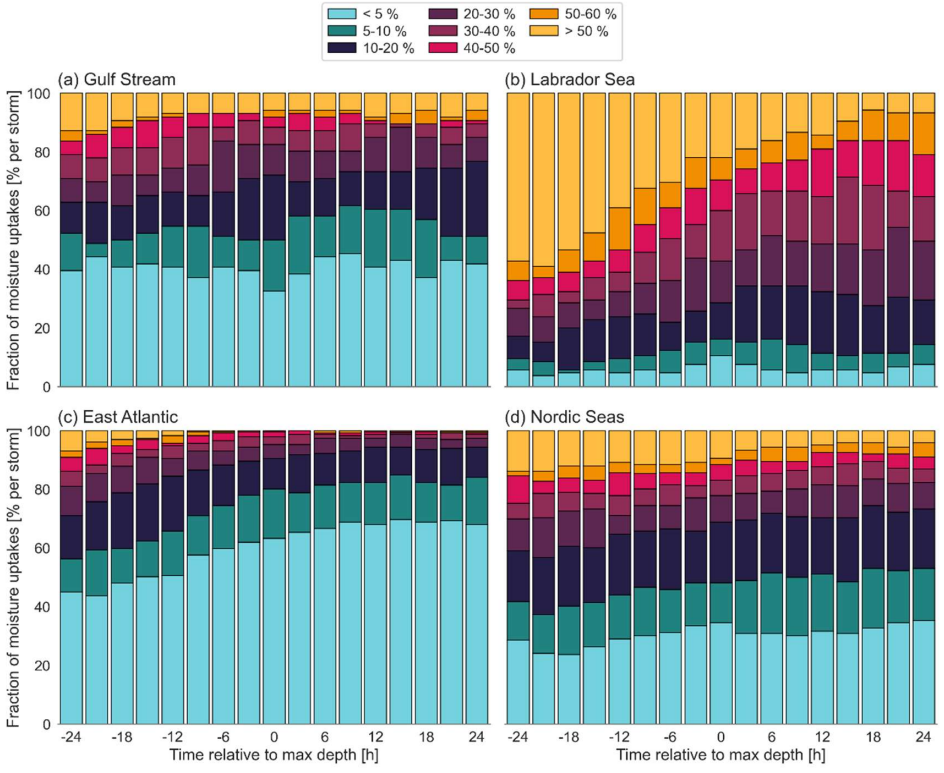

Figure A5: Uptake contributions according to the fraction of uptakes that have occurred over land, at t = -24 h to t = 24 h in 3-hourly intervals, associated with cyclones in (a) the Gulf Stream, (b) the Labrador Sea, (c) the East Atlantic, and (d) in the Nordic Seas.

Data availability. The ERA5 reanalysis data are publicly available and can be downloaded from the Copernicus Climate Change Service Data Store (https://climate.copernicus.eu/climate-reanalysis). The code used for the analysis will be made available on GitHub upon publishing [*link will be added*].

Author contributions. The main research question was conceptualized by LP and RS. The design and scope of the study were then designed by CW, IB and RS. RS performed the analysis and produced the figures, under the guidance of CW and IB. RS wrote the manuscript, with valuable feedback from FS, LP, CW and IB.

Competing interests. One of the co-authors is a member of the editorial board of Weather and Climate Dynamics. The authors declare that they have no other conflict of interest.

https://doi.org/10.5194/egusphere-2025-1752
Preprint. Discussion started: 25 April 2025

Acknowledgements. The authors would like to thank Michael Sprenger for providing the data set of cyclone tracks. We also thank Dim Coumou, Vera Melinda Galfi and Hylke de Vries for some fruitful discussions, which helped to improve this work. This study was partly funded by the European Union Horizon Europe research and innovation programme under Grant Agreement 101137656 (EXPECT project).

References

Aemisegger, F., and Sjolte, J.: A Climatology of Strong Large-Scale Ocean Evaporation Events. Part II: Relevance for the Deuterium Excess Signature of the Evaporation Flux, J. Climate, 31, 7313–7336. https://doi.org/10.1175/ JCLI-D-17-0592.1, 2018.

Ahrens, C. D.: Meteorology today: An introduction to weather, climate, and the environment, 9th ed,. Brooks/Cole, CengageLearning, ISBN 0495555738, 2009.

Bjerknes, J. and Solberg, H.: Life cycle of cyclones and the polar front theory of atmospheric circulation, Geofys. Publ., 3, 3–18, 1922.

Boutle, I. A., Beare, R. J., Belcher, S. E., Brown, A. R., and Plant, R. S.: The moist boundary layer under a mid-latitude weather system, Bound.-Lay. Meteorol., 134, 367–386, https://doi.org/10.1007/s10546-009-9452-9, 2010.

Boutle, I. A., Belcher, S. E., and Plant, R. S.: Moisture transport in midlatitude cyclones, Q. J. Roy. Meteorol. Soc., 137, 360–373, 2011.

Bui, H. and Spengler, T.: On the influence of sea surface temperature distributions on the development of extratropical cyclones, J. Atmos. Sci., 78, 1173–1188, https://doi.org/10.1175/JAS-D-20-0137.1, 2021.

Catto, J. L.: Extratropical cyclone classification and its use in climate studies, Rev. Geophys., 54, 486–520, https://doi.org/10.1002/2016RG000519, 2016.

Catto, J. L., C. Jakob, G. Berry, and Nicholls, N.: Relating global precipitation to atmospheric fronts, Geophys. Res. Lett., 39, L10805, 10.1029/2012GL051736, 2012.

Chang, E. K. M., & Song, S.: The Seasonal Cycles in the Distribution of Precipitation around Cyclones in the Western North Pacific and Atlantic. J. Atmos. Sci., 63, 815–839, https://doi.org/10.1175/JAS3661.1, 2006.

Dacre, H. F., Martinez-Alvarado, O., and Mbengue, C. O.: Linking atmospheric rivers and warm conveyor belt airflows, J. Hydrometeorol., 20, 1183–1196, 2019.

Eckhardt, S., Stohl, A., James, P., Forster, C., and Spichtinger, N.: A 15-Year climatology of warm conveyor belts, J. Climate, 17, 2018–237, https://doi.org/10.1175/1520-0442(2004)017<0218:AYCOWC>2.0.CO;2, 2004.

Field, P. R. and Wood, R.: Precipitation and cloud structure in midlatitude cyclones, J. Climate, 20, 233–254, https://doi.org/10.1175/JCLI3998.1, 2007.

Gimeno, L., Stohl, A., Trigo, R. M., Dominguez, F., Yoshimura, K., Yu, L., Drumond, A., Durán-Quesada, A. M., and Nieto, R.: Oceanic and terrestrial sources of continental precipitation, Rev. Geophys., 50, RG4003, 10.1029/2012RG000389, 2012.

https://doi.org/10.5194/egusphere-2025-1752
Preprint. Discussion started: 25 April 2025

Hersbach, H., Bell, B., Berrisford, P., Hirahara, S., Horányi, A., Muñoz-Sabater, J., Nicolas, J., Peubey, C., Radu, R., Schepers, D., Simmons, A., Soci, C., Abdalla, S., Abellan, X., Balsamo, G., Bechtold, P., Biavati, G., Bidlot, J., Bonavita, M., De Chiara, G., Dahlgren, P., Dee, D., Diamantakis, M., Dragani, R., Flemming, J., Forbes, R., Fuentes, M., Geer, A., Haimberger, L., Healy, S., Hogan, R. J., Hólm, E., Janisková, M., Keeley, S., Laloyaux, P., Lopez, P., Lupu, C., Radnoti, G., de Rosnay, P., Rozum, I., Vamborg, F., Villaume, S., and Thépaut, J.-N.: The ERA5 Global Reanalysis, Q. J. Roy. Meteor. Soc., 146, 1999–2049, https://doi.org/10.1002/qj.3803, 2020.

Knippertz, P., Wernli, H., Binder, H., Bottcher, M., Joos, H., Madonna, E., Pante, G., & Sprenger, M.: The Relationship between Warm Conveyor Belts, Tropical Moisture Exports and Atmospheric Rivers, EGU General Assembly 2018, 8–13 April 2018, EGU2018-4362, https://meetingorganizer.copernicus.org/EGU2018/EGU2018-4362.pdf, 2018

Konstali, K., Spengler, T., Spensberger, C., & Sorteberg, A.: Linking future precipitation changes to weather features in CESM2-LE. J. Geophys. Res.-Atmos., 129, e2024JD041190, https://doi.org/10.1029/2024JD041190, 2024.

Madonna, E., Wernli, H., Joos, H., and Martius, O.: Warm conveyor belts in the ERA-Interim dataset (1979–2010). Part I: Climatology and potential vorticity evolution, J. Climate, 27, 3–26, https://doi.org/10.1175/JCLI-D-12-00720.1, 2014

Laurila, T. K., Gregow, H., Cornér, J., and Sinclair, V. A.: Characteristics of extratropical cyclones and precursors to windstorms in northern Europe, Weather Clim. Dynam., 2, 1111–1130, https://doi.org/10.5194/wcd-2-1111-2021, 2021.

Lavers, D.A., Simmons, A., Vamborg, F. and Rodwell, M.J.: An evaluation of ERA5 precipitation for climate monitoring. Q. J. Roy. Meteorol. Soc., 148, 3124–3137, https://doi.org/10.1002/qj.4351, 2022.

Messmer, M. and Simmonds, I.: Global analysis of cyclone-induced compound precipitation and wind extreme events, Weather Clim. Extrem., 32, 100324, https://doi.org/10.1016/j.wace.2021.100324, 2021.

Mesquita, M. D. S., Gunnar Kvamstø, N., Sorteberg, A., and Atkinson, D. E.: Climatological properties of summertime extra-tropical storm tracks in the Northern Hemisphere. Tellus A, 60, 557–569. https://doi.org/10.1111/j.1600-0870.2008.00305.x, 2008.

Neu, U., Akperov, M. G., Bellenbaum, N., Benestad, R., Blender, R., Caballero, R., Cocozza, A., Dacre, H. F., Feng, Y., Fraedrich, K., Grieger, J., Gulev, S., Hanley, J., Hewson, T., Inatsu, M., Keay, K., Kew, S. F., Kindem, I., Leckebusch, G. C., Liberato, M. L. R., Lionello, P., Mokhov, I. I., Pinto, J. G., Raible, C. C., Reale, M., Rudeva, I., Schuster, M., Simmonds, I., Sinclair, M., Sprenger, M., Tilinina, N. D., Trigo, I. F., Ulbrich, S., Ulbrich, U., Wang, X. L., and Wernli, H.: IMILAST: A community effort to intercompare extratropical cyclone detection and tracking algorithms, B. Am. Meteorol. Soc., 94, 529–547, https://doi.org/10.1175/BAMS-D-11-00154.1, 2013.

Okajima, S., Nakamura, H., and Spengler, T.: Midlatitude oceanic fronts strengthen the hydrological cycle between cyclones and anticyclones. Geophys. Res. Lett., 51, e2023GL106187. https://doi.org/10.1029/2023GL106187, 2024.

Papritz, L., Pfahl, S., Sodemann, H. and Wernli, H.: A Climatology of Cold Air Outbreaks and Their Impact on Air–Sea Heat Fluxes in the High-Latitude South Pacific. J. Climate, 28, 342–364, https://doi.org/10.1175/JCLI-D-14-00482.1, 2015.

Papritz, L., Aemisegger, F., and Wernli, H.: Sources and transport pathways of precipitating waters in cold-season deep North Atlantic cyclones, J. Atmos. Sci., 78, 3349–3368, https://doi.org/10.1175/JAS-D-21-0105.1, 2021.

https://doi.org/10.5194/egusphere-2025-1752
Preprint. Discussion started: 25 April 2025

Pérez-Alarcón, A., Sorí, R., Fernández-Alvarez, J. C., Nieto, R., and Gimeno, L.: Where Does the Moisture for North Atlantic Tropical Cyclones Come From?. J. Hydrometeor., 23, 457–472, https://doi.org/10.1175/JHM-D-21-0117.1, 2022.

Pfahl, S., and Wernli, H.: Quantifying the Relevance of Cyclones for Precipitation Extremes. J. Climate, 25, 6770–6780. https://doi.org/10.1175/JCLI-D-11-00705.1, 2012.

Pfahl, S. and Sprenger, M.: On the relationship between extratropical cyclone precipitation and intensity, Geophys. Res. Lett., 43, 1752–1758, https://doi.org/10.1002/2016GL068018, 2016.

Pfahl, S., Madonna, E., Boettcher, M., Joos, H., and Wernli, H.: Warm conveyor belts in the ERA-Interim dataset (1979–2010). Part II: Moisture origin and relevance for precipitation, J. Climate, 27, 27–40, https://doi.org/10.1175/JCLI-D-13-00223.1, 2014.

Priestley, M. D. K. and Catto, J. L.: Future changes in the extratropical storm tracks and cyclone intensity, wind speed, and structure, Weather Clim. Dynam., 3, 337–360, https://doi.org/10.5194/wcd-3-337-2022, 2022.

Priestley, M. D. K., Pinto, J. G., Dacre, H. F. and Shaffrey, L. C.: Rossby wave breaking, the upper level jet, and serial clustering of extratropical cyclones in western Europe, Geophys. Res. Lett., 44, 514–521, 10.1002/2016GL071277, 2017.

Priestley, M.D.K., Dacre, H.F., Shaffrey, L.C., Schemm, S., Pinto, J.G.: The role of secondary cyclones and cyclone families for the North Atlantic storm track and clustering over western Europe. Q. J. Roy. Meteorol. Soc.,146,1184–1205. https://doi.org/10.1002/qj.3733, 2020.

Schultz, D. M., and Vaughan, G.: Occluded Fronts and the Occlusion Process: A Fresh Look at Conventional Wisdom. B. Am. Meteorol. Soc., 92, 443–466. https://doi.org/10.1175/2010BAMS3057.1, 2011.

Shapiro, M. A. and Keyser, D.: Fronts, jet streams and the tropopause, in: Extratropical Cyclones: The Erik Palmén Memorial Volume, edited by: Newton, C. and Holopainen, E. O., American Meteorological Society, Boston, MA, 167–191, Online ISBN 978-1-944970-33-8, 1990.

Sodemann, H.: The Lagrangian moisture source and transport diagnostic WaterSip V3.2, EGUsphere [preprint], https://doi.org/10.5194/egusphere-2025-574, 2025.

Sodemann, H., Schwierz, C., and Wernli, H.: Interannual variability of Greenland winter precipitation sources: Lagrangian moisture diagnostic and North Atlantic Oscillation influence. J. Geophys. Res., 113, D03107. https://doi.org/10.1029/2007JD008503, 2008.

Sodemann, H., and Stohl, A.: Moisture Origin and Meridional Transport in Atmospheric Rivers and Their Association with Multiple Cyclones. Mon. Wea. Rev., 141, 2850–2868, https://doi.org/10.1175/MWR-D-12-00256.1, 2013.

Sprenger, M., and Wernli, H.: The LAGRANTO Lagrangian analysis tool – version 2.0. Geosci. Model Dev., 8, 2569–2586. https://doi.org/10.5194/gmd-8-2569-2015, 2015.

Sprenger, M., Fragkoulidis, G., Binder, H., Croci-Maspoli, M., Graf, P., Grams, C. M., Knippertz, P., Madonna, E., Schemm, S., Skerlak, B., & Wernli, H.: Global Climatologies of Eulerian and Lagrangian Flow Features based on ERA-Interim. B. Am. Meteorol. Soc., 98, 1739–1748. https://doi.org/10.1175/BAMS-D15-00299.1, 2017.

https://doi.org/10.5194/egusphere-2025-1752
Preprint. Discussion started: 25 April 2025

van der Ent, R. J. and Tuinenburg, O. A.: The residence time of water in the atmosphere revisited, Hydrol. Earth Syst. Sci., 21, 779–790, https://doi.org/10.5194/hess-21-779-2017, 2017.

Weijenborg, C. and Spengler, T.: Detection and global climatology of two types of cyclone clustering, EGUsphere [preprint], https://doi.org/10.5194/egusphere-2024-3404, 2024.

Wernli, H., and Schwierz, C.: Surface Cyclones in the ERA-40 Dataset (1958–2001). Part I: Novel Identification Method and Global Climatology. J. Atmos. Sci., 63, 2486–2507, https://doi.org/10.1175/JAS3766.1, 2006.